Chromo and Fluorogenic Properties of Some Azo−Phenol Derivatives and Recognition of Hg2+ Ion in Aqueous Medium by Enhanced Fluorescence

ARTICLE *in* THE JOURNAL OF PHYSICAL CHEMISTRY C · AUGUST 2010

Impact Factor: 4.77 · DOI: 10.1021/jp1049974

2 AUTHORS:

Arvind Misra
Banaras Hindu University
48 PUBLICATIONS **447** CITATIONS
SEE PROFILE

Mohammad Shahid
Indian Institute of Technology Delhi
32 PUBLICATIONS **339** CITATIONS
SEE PROFILE

Chromo and Fluorogenic Properties of Some Azo-Phenol Derivatives and Recognition of Hg^{2+} Ion in Aqueous Medium by Enhanced Fluorescence

Arvind Misra* and Mohammad Shahid

Department of Chemistry (Centre for Advanced Study), Faculty of Science, Banaras Hindu University, Varanasi 221 005, India

Received: June 1, 2010; Revised Manuscript Received: August 14, 2010

Azo-phenol based receptors, having an azo core incorporated with naphthol and substituted (−H, $-NO_2$, $-CH_3$, and $-OCH_3$) benzothiazole units have been synthesized and their detailed optical properties have been investigated in different media. The nitro substituted azo derivative, **2**, has shown, categorically, promising optical behavior in the absence as well as presence of different transition metal ions in aqueous-acetonitrile solution and has illustrated greater sensitivity, using the "naked-eye" for the detection of Hg^{2+} ion by enhanced fluorescence. The mechanism of metal−ion interaction has been established by absorption, emission, FT-IR, and ^{1}HNMR spectroscopic experiments that indicated favorable coordination of Hg^{2+} metal ion by the phenolic oxygen atom, the azo nitrogen atom adjacent to the naphthol ring, and the thiazole nitrogen of benzothiazole ring, obviously in a terdentate manner leading to the formation of a five-membered chelate ring. The 2:1 stoichiometry and association constants, K_{assoc}(abs.) = 1.04 ± 0.3 × 10^5 M^{-2} and K_{assoc}(em.) = 1.51 × 10^5 M^{-2} have been estimated with the help of Job's plot and the Benesi−Hildebrand method. The cis−trans isomerism and azo-hydrazone type of tautomerism by the photoinduced proton transfer reaction and also metal induced (Hg^{2+} ion) proton transfer reaction from the hydrazone form in the present organic molecular systems have been confirmed by photoirradiation and fluorescence excitation experiments and by ^{1}H and ^{13}C NMR spectral analysis.

Introduction

Considerable current interest has arisen in the design and synthesis of simple and efficient chemosensors of high selectivity and sensitivity for the recognition of biologically important and toxic metal ions in the area of supramolecular chemistry.[1] Among the various heavy and transition metal ions and an increasing threat of mercury[2] exposure in the environment from global mercury emissions and a variety of contaminations,[3−5] there has been growing interest in the development of specific molecular systems for mercuric (Hg^{2+}) ions. The accumulation of mercury in the human body may cause serious health problems like prenatal brain damage, cognitive and motion disorder, Minamata diseases, etc.[6,7] Similarly, copper has also been considered as a biologically important transition metal ion[8] because its higher concentration may displace other metal ions and/or cofactors that are useful for various biologically important enzyme catalyzed chemical reactions.[9] The fluctuations in Cu^{2+} ion concentration may also induce oxidative stress and their infection in neuronal cytoplasm may cause Alzheimer's or Parkinson's disease.[10]

The development of colorimetric sensors for the detection of heavy and transition metal ions are increasingly appreciated important aspect since "naked-eye" detection may offer qualitative and quantitative information. In this direction, various sensor systems based on organic chromophores,[11] redox potentials,[12] fluorophores,[13] and nanomaterials[14] have been developed. Most of the systems explored so far in the recognition of metal ions however, have some limitations in terms of sensitivity, selectivity, and simplicity. The known reversible chemosensors generally work well in organic and/or aqueous (or mixed with organic cosolvent) medium, and also some of them are efficient in strong acidic or alkaline pH conditions.[15] Additionally, in most of the sensory systems that work well in the organic medium, the sensing events revert back upon the addition of competitive solvents such as water. Therefore, development of a sensitive, reliable, concurrent, cost-effective, and aqueous medium compatible optical systems are in high demand for the detection of heavy and transition metal ions, particularly for the mercury ion contamination in water and the environment. In this prospective some specific chemosensors based on organic molecular systems/materials have been developed for the detection of Hg^{2+}/Cu^{2+} metal ions, to include, azo-derivatives,[16] *N*-dansylcarbaxamide,[17] aminonaphthol,[18] anthrylacetamide,[19] crown-ethers,[20] thiocarbamate,[21] naphthalimides,[22] rhodamine,[23] anthraquinone,[24] benzothiazole,[25] fluorescein,[26] etc.

Further, most of the heavy and transition metal ions generally cause nonspecific fluorescence quenching upon interaction with probe/receptor molecules. For example, Hg^{2+} and paramagnetic Cu^{2+} metal ions generally induce fluorescence quenching due to enhanced spin−orbit coupling[27] and by energy or electron transfer mechanism,[28,29] respectively. Thus, a receptor having both chromo and fluorogenic properties and that is sensitive to changes in their optical properties[30] selectively, in the presence of metal ions like mercury, will be interesting in naked-eye visible recognition events.[31] Moreover, those molecular systems which are capable in chelate formation will have added advantages with respect to obtaining better fluorescence responses and to monitor such metal ions by the possible chelation-enhanced quenching (CHEQ) or chelation-enhanced fluorescence (CHEF) mechanism.[32−34]

Keeping the above facts in mind, we have synthesized some azo-phenol derivatives, **2**−**6** having an azo core, incorporated

* Corresponding author. E-mail: arvindmisra2003@yahoo.com; amisra@bhu.ac.in. Tel.: +91-542-2307321 ext. 104; +91-542-6702503. Fax: +91-0542-2368127, 2368175.

10.1021/jp1049974
Published on Web 09/01/2010

between the naphthol and substituted benzothiazole units, and carried out detailed photophysical studies in different solvent systems including surfactant medium, in the absence as well as presence of different metal ions categorically in aqueous-acetonitrile solution (ACN/H_2O; 1:1; *v*/*v*). We tried to explain and establish the cis−trans photoisomerism and azo-hydrazone type of tautomerism in the present organic molecular systems and also about the specific change occurred in the optical properties as a consequence of probable complexation reaction with different metal ions. The manuscript also emphasizes about the significance of geometric configuration and structural changes occurred in the recognition of metal ions by the absorption and emission spectroscopic data. The azo derivative, **2** has shown better optical behavior and was found most suitable, selective, and also 'naked-eye' sensitive in the detection of Hg^{2+} metal ion. The mechanism of metal ion interaction has been confirmed by ^1H NMR titration experiments. FT-IR spectral analysis up to some extent, have also suggested about the mode of interaction with Hg^{2+} metal ion.

We assumed that due to the presence of various donor sites in the form of N, S, and O atoms, azo hydrazo type systems would behave as a potential ligand, and upon interaction with different metal ions, specifically the Hg^{2+} metal ion would led to the formation of a metal−ligand complex in a specific stoichiometry. Moreover, the extended π-conjugation and appended azo chromophore will be useful in obtaining significant and detectable optical signals, both the absorption and emission, and would show some significant metal assisted variations in their optical property utilizing the specific mechanisms of photophysics, consequently the prominent color changes in the medium would remarkably facilitate the naked-eye detection of metal ions.

Experimental Section

General. IR spectra in KBr were recorded on a Varian-3100 and JASCO-5300 FT-IR spectrometer. ^1H NMR spectra (chemical shifts in δ ppm) were recorded on a JEOL AL 300 FT-NMR (300 MHz) spectrometer, and ^{13}C NMR spectra (chemical shifts in δ ppm) were recorded at 75 MHz on the same FT-NMR spectrometer, using TMS as internal standard. The UV−vis absorption spectra were recorded on Shimadzu 1700 spectrophotometer using a quartz cuvette of 1 cm path length and was scanned from 200 to 700 nm wavelengths keeping constant slit width through out the whole experiments. Fluorescence spectra were recorded in a 3 and 1 mL screwed Hellma cuvettes on a Cary Eclipse spectrofluorometer keeping a constant slit width 5/5 nm at excitation and emission sites respectively, utilizing 600 V, PMT. The pH was measured on CyberScan pH1100, pH/mV/°C/F meter with RS232 (Eutech Instruments, Merck India Pvt. Ltd.). To measure the pH of the azo-phenol derivatives **2**, **5**, and **6**, two methods have been adopted as reported previously.[26]

Method I. A 25 mL stock solution of 4×10^{-5} M concentration of derivatives **2**, **5**, and **6** was prepared in acetonitrile, because these compounds were sparingly soluble in water. To the 5 mL solution of derivatives **2**, **5**, and **6** in ACN, 5 mL of 0.5 M HCl solution was added to get a 10 mL stock solution of 2×10^{-5} M concentration in ACN/H_2O (1:1) mixed solvent system. The pH 1−12 was maintained by the addition of calculated amount of aqueous 1 M NaOH solution (∼10 μL) to the solution of the derivatives, consequently forming a B/BH^+ buffer in the system. The solution was stirred for 3−5 min, and pH was recorded with the help of a digital precalibrated pH meter and then absorption and emission spectra were measured at a particular pH.

Method 2. To the 5 mL solution of different derivatives **2**, **5**, and **6** (4×10^{-5} M) 5 mL HCl solution of concentrations, 0.5, 0.05, 0.01, 0.005, and 0.001 M were added, and the resulting ACN/H_2O solution was stirred for 3−5 min. The prepared stock solutions for each derivative individually have shown pH 1, 3, 4, 5, and 6, respectively. To maintain pH 5−12, a calculated amount of aqueous 1 M NaOH solution was added to the solution of different derivatives, consequently making B/BH^+ buffer in the system and then both the absorption and fluorescence spectra were measured.

For Intermolecular Charge Transfer (CT) Transition. For the study of intermolecular charge transfer transition, a stock solution of **2** of 1×10^{-3} M concentration in DMSO was prepared and was diluted to get 0.5, 1.0, 2.0, 2.95, 3.8, 4.7, 5.6, 6.5, 7.4, 8.2, 9.0, 9.9, 10.7, 11.5, 12.2, 13.0, 13.7 14.5, and 15.3×10^{-5} M solution of **2** in DMSO. UV−vis spectra of different concentrations were recorded, and a plot was taken between absorbance vs concentrations. Similarly, in an attempt to observe the effect of DMSO in inducing proton transfer by the complexation reaction, another experiment was designed by increasing the concentration of DMSO (0.64, 1.28, 1.92, 2.56, 3.2, 3.84, 4.5, 5.1, 5.8, 6.4, 7.0, 7.7, 8.3, 9.0, 9.6, and 10.2 mM) to the solution of **2** in acetonitrile, and absorption spectra were recorded.

General Method for Synthesis of Benzothiazole Derivatives. The substituted benzothiazole was synthesized by a previously reported method.[35] The *p*-substituted anilines (15 mmol) were taken in acetic acid (10−15 mL), and the solution of potassium thiocyanate (60 mmol, 5.8 g) in acetic acid (20 mL) was added. The reaction mixture was stirred for 30 min at room temperature and then cooled to 0−5 °C. To the cold solution was added dropwise for 30 min a bromine solution (16 mmol, 0.8 mL) in acetic acid (10 mL). The reaction mixture was allowed to reach room temperature and stirred for 22 h. After completion of the reaction (monitored on TLC), cold water was added to the reaction mixture for precipitation and filtered. The precipitate so obtained was suspended in water and neutralized with ammonia (30%) solution, filtered, washed with water (3 × 10 mL), and dried to get the 6-substituted 2-aminobenzothiazoles (**1**) in ∼67 − 79% yield.

2-Amino-benzothiazole (1a). Yield 79% (11.8 mmol, 1.77 g); mp 133−135 °C; R_f 0.31 (EtOAc:hexane, 4:6 *v*/*v*); ^1H NMR (DMSO-d_6, 300 MHz) δ 8.08 (1H, d, $J = 6.6$ Hz), 7.83 (2H, s, NH_2), 7.50 (t, 1H, $J = 1.6$, 6.6 Hz), 7.741(2H, d, $J = 8.4$ Hz); ν_{max} (KBr): 3396, 3270, 1641, 1625, 1593, 1532, 1449, 1315, 1172, 885, 743 cm^{-1}; Anal. Calc. for $C_7H_6N_2S$; C, 55.97; H, 4.03; N, 18.65%. Found: C, 55.71; H, 4.10, N, 18.79%.

2-Amino-6-nitrobenzothiazole (1b). Yield 67% (10.1 mmol, 1.96 g); mp 249−253 °C; $R_f = 0.42$ (EtOAc:hexane, 1:1 *v*/*v*); ^1H NMR (DMSO-d_6, 300 MHz) δ 8.68 (1H, d, $J = 2.1$ Hz), 8.23 (2H, s, NH_2), 8.11 (1H, dd, $J = 9.0$, 2.4 Hz), 7.42 (1H, d, $J = 9.0$ Hz); ν_{max} (KBr): 3460, 3292, 1628, 1573, 1532, 1494, 1333, 1296, 889, 821, 753 cm^{-1}; Anal. Calc. for $C_7H_5N_3O_2S$; C, 58.51; H, 4.91; N, 17.06%. Found: C, 57.97; H, 4.99, N, 17.13%.

2-Amino-6-methylbenzothiazole (1c). Yield 72% (10.8 mmol, 1.77 g); mp 142−144 °C; $R_f = 0.34$ (EtOAc:hexane, 4:6 *v*/*v*); ^1H NMR (DMSO-d_6, 300 MHz) δ 7.93 (2H, s, NH_2), 7.58 (1H, s), 7.45 (1H, d, $J = 6.6$ Hz), 7.22(1H, d, $J = 8.4$ Hz), 2.35 (3H, s, CH_3); ν_{max} (KBr): 3390, 3262, 1632, 1621, 1569, 1540, 1280, 811, 725 cm^{-1}; Anal. Calc. for $C_8H_8N_2S$; C, 58.51; H, 4.91; N, 17.06%. Found: C, 57.97; H, 4.99, N, 17.13%.

2-Amino-6-methoxybenzothiazole (1d). Yield 74% (11.1 mmol, 1.99 g); mp 166−168 °C; R_f = 0.33 (EtOAc:hexane, 4:6 *v*/*v*); ^{1}H NMR (DMSO-d_6, 300 MHz) δ 7.78 (2H, s, NH_2), 7.52 (1H, s), 7.42 (1H, d, J = 6.6 Hz), 6.92 (d, 1H, J = 6.6 Hz), 3.73 (3H, s, OCH_3); ν_{max} (KBr): 3398, 3282, 2912, 1635, 1615, 1553, 1472, 1390, 1282, 1210, 1075, 1025, 851, 735 cm^{-1}; Anal. Calc. for $C_8H_8N_2OS$; C, 53.31; H, 4.47; N, 15.54%. Found: C, 52.97; H, 4.59, N, 15.63%.

General Procedure for the Synthesis of Receptors. 2-Amino-6-substituted benzothiazoles (1.0 mmol) were dissolved in acetic acid (3.8 mL) containing concentrated sulphuric acid (2.2 mL) and cooled to 0−5 °C in an ice bath. The ice-cold solution of $NaNO_2$ (1.4 mmol, 0.097 g) in water (0.3 mL) was added dropwise to the reaction mixture with constant stirring to obtain the diazonium salt, **1a**−**d**. After complete addition the resultant mixture was left in an ice chest for 1 h, and alkaline β-naphthol (1.0 mmol, 0.144 g) solution was added dropwise to the ice-cold solution of **1** to obtain dark reddish brown colored azo compounds **2**−**6** which, upon addition of more alkaline β-naphthol solution, become darkened. After complete addition, the reaction mixture was further stirred for 2 h and then filtered. The residue was washed comprehensively with water, dried, and again washed with methanol (3 × 5 mL) and crystallized in chloroform.

6-Nitrobenzothiazole Derivative (2). Yield 72% (0.72 mmol, 0.25 g). mp 107 °C; R_f = 0.3 (EtOAc:hexane, 4:6 *v*/*v*); ^{1}H NMR ($CDCl_3$, 300 MHz) δ 15.79 (1H, br, N−H), 8.71 (1H, s, benzothiazole), 8.37 (2H, t, J = 8.4, 7.2 Hz, naphthyl), 7.89 (1H, d, J = 9.0 Hz, benzothiazol), 7.73 (1H, d, J = 9.6 Hz, naphthyl), 7.62 (1H, m, naphthyl), 7.51 (2H, m, 1H naphthyl and 1H benzothiazole), 6.68 (1H, d, J = 9.9 Hz naphthyl); ^{13}CNMR ($CDCl_3$, 75 MHz) δ 181.0, 153.3, 145.0, 134.5, 130.3, 129.7, 129.4, 129.0, 128.8, 127.7, 126.4, 126.3, 125.9, 123.5, 122.3, 121.6, 117.7, 109.4; ν_{max} (KBr): 3431, 1622, 1572, 1522, 1446, 1335, 1280, 1170, 832, 754, 677, 479 cm^{-1}; Anal. Calc. for $C_{17}H_{10}N_4O_3S$; C, 58.28; H, 2.88; N, 15.99%. Found: C, 57.71; H, 3.01, N, 16.05%.

Synthesis of Compound 3. Compound **2** (0.1 mmol, 35 mg) was dissolved in dry acetone, and K_2CO_3 (0.2 mmol, 28 mg) and methyl iodide (0.5 mmol, 71 mg) were added, and the reaction mixture was refluxed for 4−5 h. After completion of the reaction (monitored on TLC), the reaction mixture was cooled in an ice bath and dried under vacuum. The product was washed with water and dried to obtain brown-colored compound **3** which was crystallized with methanol to obtain the desired compound as brown-colored powder in 86% (0.086 mmol, 43 mg) yield, mp 95 °C. R_f = 0.2 (EtOAc:hexane, 3:7 *v*/*v*); ^{1}H NMR ($CDCl_3$, 300 MHz) δ 8.87 (1H, s, benzothiazole), 8.29 (2H, m, naphthyl), 8.02 (1H, m, naphthyl), 7.84 (2H, dd, J = 8.7 Hz, 1H benzothiazole and 1H naphthyl), 7.54 (2H, dd, J = 9.3 Hz, 1H benzothiazole and 1H naphthyl), 7.12 (1H, naphthyl, overlapped with signal of $CDCl_3$ solvent), 3.92 (3H, s, - OCH_3), 3.28 (3H, s, -NCH_3); ^{13}CNMR ($CDCl_3$, 75 MHz) δ 148.5, 145.9, 139.5, 139.2, 138.1, 129.3, 127.6, 126.7, 126.3, 125.6, 123.5, 122.7, 118.6, 118.6, 10.9, 105.7, 55.2, 29.6; ν_{max} (KBr) 1627, 1438, 1335, 1095, 1028, 799, 680, 475 cm^{-1}; Anal. Calc. for $C_{19}H_{15}N_4O_3SI$; C, 45.07; H, 2.99; N, 11.07%. Found: C, 45.53; H, 3.10, N, 11.14%.

6-Hydrobenzothiazole Derivative (4). Yield 75% (0.75 mmol, 0.23 g). mp 162 °C; R_f = 0.35 (EtOAc:hexane, 2:8 *v*/*v*); ^{1}H NMR ($CDCl_3$, 300 MHz) δ 15.70 (0.3H, br, N−H), 15.55 (0.6H, br, O−H), 8.40 (1H, d, J = 7.8 Hz), 7.93 (1H, m), 7.87 (1H, d, J = 8.4 Hz), 7.83 (1H, d, J = 8.4 Hz), 7.73 (1H, d, J = 9.6 Hz), 7.62 (3H, m), 7.47 (1H, d, J = 6.9 Hz), 6.76 (1H, d, J = 9.6 Hz); ^{13}CNMR ($CDCl_3$+DMSO-d_6, 75 MHz) δ 178.1, 152.3, 143.8, 142.9, 133.5, 132.6, 132.0, 131.3, 129.5, 128.7, 128.5, 127.8, 124.8, 124.1, 123.6, 122.7, 122.4; ν_{max} (KBr): 3439, 3229, 3138, 1626, 1496, 1390, 1315, 1259, 1174, 872, 771, 522 cm^{-1}; Anal. Calc. for $C_{17}H_{11}N_3OS$; C, 66.87; H, 3.63; N, 13.76%. Found: C, 66.70; H, 3.71, N, 13.91%.

6-Methylbenzothiazole Derivative (5). Yield 70% (0.7 mmol, 0.22 g). mp 93 °C; R_f = 0.57 (EtOAc:hexane, 2:8 *v*/*v*); ^{1}H NMR ($CDCl_3$, 300 MHz) δ 15.58 (1H, br, OH), 8.39 (1H, d, J = 7.5 Hz), 7.74 (1H, d, J = 9.6 Hz,), 7.58 (6H, m), 6.76 (1H, d, J = 6.6 Hz), 2.52 (3H, s); ^{13}CNMR ($CDCl_3$+DMSO-d_6, 75 MHz) δ 172.4, 167.9, 143.2, 141.8, 135.5, 132.6, 132.1, 129.3, 128.5, 128.3, 127.4, 126.6, 124.3, 123.2, 122.1, 121.5, 120.8, 116.2, 110.4, 20.8; ν_{max} (KBr): 3408, 3273, 1687, 1618, 1489, 1466, 1398, 1271, 1248, 1151, 906, 837, 761 cm^{-1}; Anal. Calc. for $C_{18}H_{13}N_3OS$; C, 67.69; H, 4.10; N, 13.16%. Found: C, 66.78; H, 4.21, N, 13.25%.

6-Methoxybenzothiazole Derivative (6). Yield 68%, (0.68 mmol, 0.23 g). mp 135−138 °C; R_f = 0.55 (EtOAc:hexane, 2:8 *v*/v); ^{1}H NMR ($CDCL_3$, 300 MHz) δ 15.38 (s, 1H), 8.43 (d, 1H, J = 8.4 Hz), 7.78 (d, 1H, J = 9.6 Hz), 7.59 (d, 2H, J = 4.5 Hz), 7.49 (m, 2H), 7.30 (m, 2H), 6.84 (1H, d, J = 9.6 Hz), 3.93 (s, 3H, OCH_3);^{13}CNMR ($CDCl_3$+DMSO-d_6, 75 MHz) δ 167.4, 157.3, 155.0, 142.4, 134.8, 132.0, 130.0, 129.8, 129.1, 127.8, 126.9, 124.4, 123.4, 119.5, 105.0, 55.4; ν_{max} (KBr): 3395, 3270, 1647, 1619, 1490, 1463, 1391, 1275, 1245, 1155, 1077, 1028, 841, 755 cm^{-1}; Anal. Calc. for $C_{18}H_{13}N_3O_2S$; C, 64.46; H, 3.91; N, 12.53%. Found: C, 63.95; H, 4.05, N, 12.70%.

Results and Discussion

Synthesis and ^{1}H and ^{13}C NMR Spectra Analysis. The azo phenol systems are interesting and are supposed to exist in the dynamic equilibrium of azo-hydrazone tautomerism in both solutions and solid phases in which the hydrazone form thermodynamically dominates over the azo form.[36] The predominance of one tautomeric form over the other is basically guided by the orientation effects of substituents attached to the aromatic units. The hydrazone form dominates in the presence of electron withdrawing groups at any one of two conjugating units. On the other hand, in the presence of electron releasing groups and in simple phenols and if the dynamic equilibrium prevails between the two tautomers, the azo form dominates in the medium.[37] The azo-phenol conjugated system involving naphthol and benzothiazole derivates behaves differently. Unsubstituted naphthol or naphthol appended with electron withdrawing groups intimidate such type of organic systems to exist predominately in the hydrazone form, and if a dynamic equilibrium prevails in the medium, equilibrium tends to the favor hydrazone rather than the azo form.

In view of the above-mentioned facts and for better optical signals, azo derivatives **2**−**6** have been synthesized from different derivatives of the primary aromatic amine (Scheme 1) by previously reported method[35] and characterized. The azo derivatives **2**−**6** have been characterized by ^{1}H NMR spectra in $CDCl_3$ solution (Figure S1−S7, Supporting Information). The chemical shifts for resonance signals of the aromatic protons appeared in between δ 8.5 and 6.5. The azo derivative **2** (c = 1.14 × 10^{-2} M) containing an electron withdrawing nitro substituent at the C-6 position of benzothiazolyl (BT) unit shows a characteristic signal (Figure S1) at δ 15.79 while derivatives **5** and **6** containing the electron donating, methyl and methoxy groups at C-6 of BT unit, have shown specific chemical shifts at δ 15.5 and 15.38 respectively (Figure S6 and S7). However, compound **4** which does not contain any substituent at the

SCHEME 1: (i) AcOH/KSCN/Br_2/0 °C to RT/Δ (ii) AcOH/H_2SO_4/$NaNO_2$/0−5 °C (iii) alk. β-Naphthol/0−5 °C (iv) MeI/K_2CO_3/dry acetone/4−5h

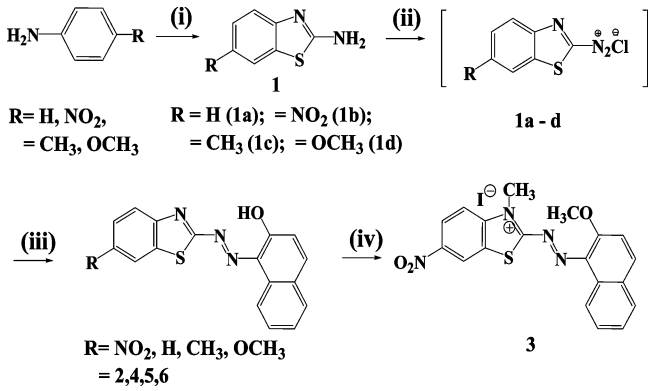

benzothiazolyl unit has illustrated two close magnetic resonance signals at δ 15.7 and 15.5. The resonance signals significantly appeared in the low field region may be assigned to a phenolic, OH and/or hydrazone, NH protons and is presumably due to the hydrogen bonding between azo and hydroxyl chromophore through a probable six-member cyclic transition state and/or also may be due to the interaction of π electrons of aromatic rings arranged in geometrically trans configuration. The two close chemical shifts, at 15.7 and 15.5 δ, observed in the case of compound **4** may be attributed to the NH and OH protons, respectively, and therefore suggested the existence of azo-hydrazone type of tautomerism in the medium. To get an idea about the percentage of existence of tautomers in the medium, in the case of **4**, the peak areas of probable chemical shifts corresponding to both the hydrazone and the azo forms were roughly estimated and found to be ∼31% and ∼69%, respectively. However, derivatives **2**, **5**, and **6**, in spite of containing electron withdrawing (−NO_2) and donating (−CH_3 and −OCH_3) substituents at BT unit, were found to exist dominantly in the hydrazone form which is evidenced by the appearance of sharp resonance signals at δ 15.79, δ 15.5, and δ 15.38, respectively, in the ^{1}H NMR spectra. When the solution of **2** was treated with D_2O solution, the observed downfield chemical shifts in the ^{1}H NMR spectra disappeared, therefore, further supporting the attributed signals for either azo (−OH) and/or hydrazone (−NH) proton (Figure S8, Supporting Information).

Further analysis of ^{13}CNMR data of derivatives, **2**, **4**, **5**, and **6** have been carried out to understand the existence of the azo-hydrazone type of tautomerism in the medium. The unsubstituted azo-phenol derivative **4** shows resonance signals for the C−O carbon around δ 178 ppm corresponding to the keto form[36b] and signals in the range of δ 140−155 ppm are typical for a C−O(H) functionality,[36c] thus suggesting the existence of the azo-hydrazone tautomeric forms in the medium.[36d,e] In an investigation to observe the effect of substituents incorporated at the C6 position of the BT unit, the ^{13}CNMR spectrum of **2** containing the electron withdrawing −NO_2 substituent was analyzed, and that shows signals corresponding to the both keto and enol forms, which was slightly shifted in the low field region. The azo-phenol derivatives **5** containing the electron donating substituent −CH_3 have illustrated resonance signals at δ 172.4 and at δ 167.9 ppm, whereas in case of the −OCH_3 derivative **6**, resonance signals appeared at δ 167.4 and in the range of δ 155−158 ppm. The relative high and low field chemical shifts at the corresponding hydrazone (keto) and azo (enol) forms clearly indicated the existence of a dynamic equilibrium between the azo-hydrazone tautomeric forms, in

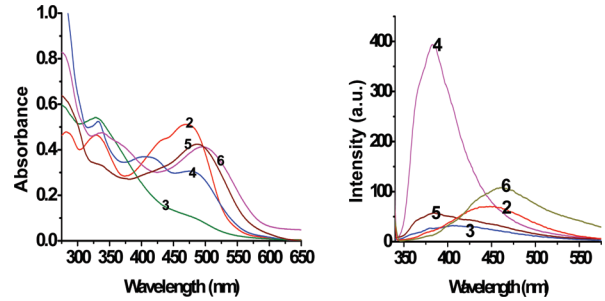

Figure 1. UV−vis and fluorescence spectra for **2**−**6** in ACN/H_2O mixed solvent system.

which the hydrazone form dominates, as substantiated by ^{1}HNMR spectral analysis.

Photophysical Properties of Synthesized Azo Derivatives. The UV−vis spectrum of **2** shows the low energy bands ($n \rightarrow \pi^*$) at 474 nm with a broad shoulder at 435 nm and a high energy band ($\pi \rightarrow \pi^*$) at 332 nm. The bands corresponding to electronic transitions, $n \rightarrow \pi^*$, may be assigned due to the hydrazone and azo tautomers in the medium, in which the hydrazone isomer dominates (Figure 1). The prominent high energy band due to the $\pi \rightarrow \pi^*$ electronic transition has suggested the existence of **2** predominantly in the geometrically trans configuration.[38] The absorption spectrum of **4** shows bands at 474, 408, and 335 nm. The molar extinction coefficient ratio corresponding to both low and high energy electronic transitions indicates the existence of **4** in the equilibrium of both azo-hydrazone tautomeric forms, in which the percentage of azo form is relatively more and attains the trans configuration. However, the low energy $n \rightarrow \pi^*$ electronic transition band in the absorption spectrum of **5** has shown a shift toward the longer wavelength region and appeared at 493 nm with a broad shoulder at 435 nm. Similarly derivative **6** containing −OCH_3 substituent at BT unit shows absorption maxima at 496 nm and broad band around 338 nm. However, in case of **5** the high energy absorption band appeared at 335 nm wavelength was less prominent, that can be assumed for less stability for trans (*E*) isomer in the medium. To confirm the trans configuration in the synthesized derivatives, the *N*/*O*-methyl derivative **3** has been synthesized and is envisaged by the appearance of only high energy $\pi \rightarrow \pi^*$ electronic transition band at 335 nm, whereas the other electronic transition bands, such as $n \rightarrow \pi^*$, were restricted due to the methylation of active donor sites (Figure S14, Supporting Information), and that also inhibits the coherence of azo-hydrazone tautomerism in the medium. Additionally, the low energy band may be of considerable charge transfer character that would probably originate from phenolic unit to high electron accepting heterocyclic benzothiazole (BT) ring. The position and molar extinction coefficient of the bands may be highly influenced by the nature of polar substituents (+*I*/−*I* effect) present on the BT unit. Comparatively, the more red-shift in the absorption spectra of **5** and **6** than of **2** can be accounted for by considering the greater delocalization of the electrons in th ecase of **2** and by the antagonizing effect of the electron releasing substituents.[46]

The fluorescence intensity measurement for receptors **2**, **4**, and **5** in the absence and presence of different metal ions was carried out in aqueous acetonitrile solvent mixture (H_2O/ACN; 1:1). In the absence of metal ion receptors, **4** and **5** upon excitation at 334 and 300 nm have shown an emission band around 385 nm, in which relatively higher fluorescence intensity for **4** was observed. Similarly, **2** upon excitation at 334 nm have emitted a weak fluorescence band at 447 nm with a relatively

greater Stoke's shift of 113 nm. The large Stoke's shift and weak fluorescence observed in the case of azo phenol derivatives **2** and **5** can be understood with the strength of inductive effects generated by the presence of $-NO_2$ and $-CH_3$ substituents, respectively.

cis−trans Photoisomerization and Azo-Phenol Tautomerism. The azo derivatives are supposed to demonstrate cis−trans isomerism on photoirradiation reaction and usually exist in different tautomeric forms.[38] The presence of at least one protic donor group in conjugation to the azo bridge helps in establishing a prototropic equilibrium that, increases the probability for the existence of azo-hydrazone tautomerism in the medium. In order to understand the potentiality for such phenomena in the present study, the solutions of azo derivatives **2**, **4**, and **5** were prepared (2×10^{-5} M) in an aprotic solvent, tetrahydrofuran (THF), and were taken in a sealed 1 cm path length quartz cuvette. Each vial was given UV exposure of 365 nm wavelength for a constant period of time (30 s) at room temperature with the help of a UV lamp (GeNei). After each UV exposure, at regular interval of time, the absorption spectra were measured on a UV−vis spectrophotometer. The change in extinction coefficient corresponding to the predicted transition bands were estimated and utilized to know the rate as well as fraction for cis isomer, generated in the medium. The same experiment was also utilized to estimate the percentage of azo and hydrazone tautomers with the help of following equations[39] (1) and (2), respectively:

$$Y = (1 - A/A_0)/(1 - \varepsilon_{cis}/\varepsilon_{trans}) \quad (1)$$

and

$$K_T = [H]/[A] = \varepsilon_M - \varepsilon_A/\varepsilon_H - \varepsilon_M \quad (2)$$

where Y stands for the fraction of cis isomer generated in the medium, A_0 is the initial absorbance for trans isomer only, A is the absorbance after each UV irradiation, and $\varepsilon_{cis}/\varepsilon_{trans}$ is the ratio of molar absorption coefficient for cis and trans isomers. The concentration of hydrazone and azo isomers is represented by [H] and [A], and ε_M stands for extinction coefficient for mixed species in the medium.

Upon photoirradiation, the absorption spectrum of **2** was steadily modulated, in which the extinction coefficients corresponding to both high ($\pi \rightarrow \pi^*$) and low energy ($n \rightarrow \pi^*$) electronic transition bands, at 332 and 472 nm wavelengths, attributed to trans and hydrazone isomer respectively were decreased. After 490 s of photoirradiation, the low energy band was completely disappeared and concomitantly, a new band attributed to azo isomer was appeared at 417 nm wavelength. The time vs photoisomerization plot was obtained to estimate the fraction for cis isomer (Y) generated in the medium. It was interesting to observe that after 8 min of photoirradiation azo derivative **2** slowly undergo configuration change to generate ~32% *cis* isomer (Figure 2 I) and color of the solution was changed from an orange brown to yellow.

Similarly, for derivatives **4** and **5** the time vs Y plots were also obtained after each photoirradiation at regular time intervals (Figure 2 II). Upon UV irradiation, the absorption bands for unsubstituted azo derivative **4** at 335 and 409 nm were reduced gradually; however, no significant modulation at 480 nm was observed (Figure S9). Interestingly, the rate of conversion for geometrically trans to cis isomer was rapid and ~39% cis isomer was generated in 6 min of UV exposure. When the number of

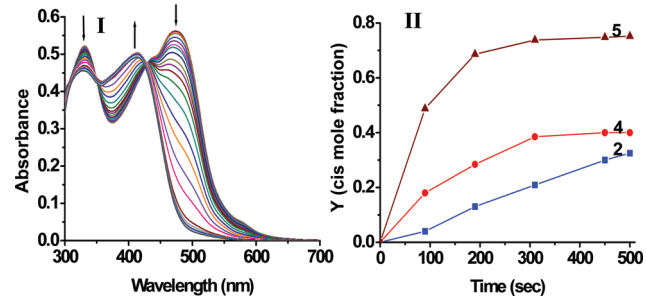

Figure 2. (I) Change in UV−vis absorption spectra for **2** after photoirradiation by UV light (at 365 nm). (II) Kinetics graph of **2**, **4**, and **5** showing photoisomerization from trans to cis with respect to time (in seconds).

photoirradiations was increased, the rate of photoisomerization reaction for the cis isomer slows down and becomes constant. However, the equilibrium corresponding to both azo-hydrazone tautomerism, in which the azo form dominates (64%), gets converted almost completely in the hydrazone form (100%). Similarly, azo derivative **5** (methyl at C-6) consisting of 0.65 mol fraction for hydrazone rapidly undergoes photoisomerisation reaction to generate ~74% cis isomer in 6 min of UV exposure, and the percentage of azo form was increased (Figure S9). The complete disappearance of high energy band, attributed to hydrazone, in 10 min of photoirradiation in the case of **2** and the change in the ratio of azo and hydrazone tautomerism for **4** and **5** have clearly suggested azo-hydrazone tautomerism and is probably due to the photoinduced proton transfer reaction[40] and/or inductive effect, put forth by the $-NO_2$, $-H$, $-OCH_3$, and $-CH_3$ groups present on the benzothiazole unit of azo derivatives respectively. Thus, the time kinetics study has revealed the stability and existence of derivative **2** dominantly in the trans configuration.

The photoisomerization event in the case of **2** and **5** has been further realized by the relative change in the intensity signals of emission spectra in THF. After photoirradiation for stipulated time intervals, as mentioned above, the emission spectra were measured by exciting the molecules **2** and **5** corresponding to their both hydrazone and azo absorption maxima. In THF, **2** at 332 nm excitation shows an emission band at 436 nm along with shoulders at 530 and 387 nm. After each photoirradiation, a gradual increase in the relative fluorescence intensity was observed in which the emission band centered at 436 nm was red-shifted for 47 nm to appear at 583 nm. Similarly, when **2** was excited at 472 nm a weak emission band centered around 562 nm, due to the diverse isomerization reaction and forbidden $n \rightarrow \pi^*$ electronic transition state of the trans isomer[38] was observed, which upon photoirradiation for a total 600 s was blue-shifted to appear at 536 nm wavelength with a shift of 26 nm. For **5** insignificant change in the relative fluorescence intensity was observed when excited at the absorption maximum corresponding to the hydrazone form; however, a gradual rise in the intensity signal was observed when **5** was excited at the high energy band (Figure 3). The observed change in the fluorescence intensity signal can be rationalized for a change in the geometrical configuration from trans to cis and/or also due to the dynamic change in the azo-hydrazone tautomerism and vice versa as a consequence of the photoinduced proton transfer reaction.[40] The advantage of exciting the molecule at low energy band is understood, and in fact by doing so the azo chromophore would remain in the ground state and the hydrazone unit will absorb more energy to reach the molecule in the excited state.

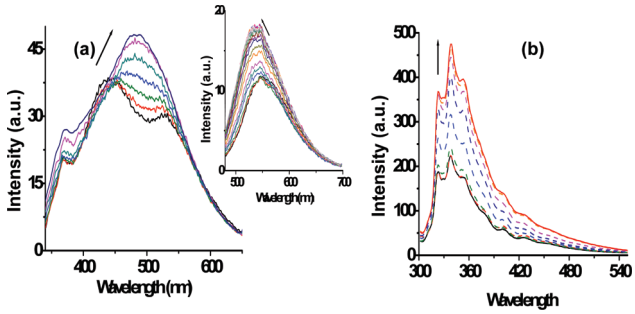

Figure 3. Panels a and b show change in fluorescence intensity of **2** and **5**, respectively, after each photoirradiation. The inset shows change in fluorescence intensity at $\lambda_{ex} = 472$ nm.

SCHEME 2

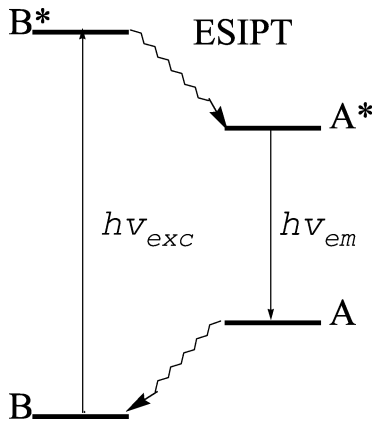

The photoinduced electron and proton transfer are fundamental processes and generally exhibited by a number of natural systems, including azo-phenol systems. The excited state intramolecular proton transfer[40] (ESIPT) and photoinduced proton transfer[41] processes are of tremendous interest because of their importance in the design and development of organic molecular devices.[42] Particularly, the ESIPT process involves the intramolecular hydrogen bond present between the closely obtainable acidic and basic groups in the ground state (Scheme 2). Upon excitation to the first excited state, because of change in the charge density and increase in acidity and basicity of the two complementary centers ultrafast migration of a proton through a hydrogen bond coordinate is possible to develop a phototautomer. Also the occurrence of ESIPT accompanied by large changes of dipole moment is difficult to comprehend, since a proton transfer event can be influenced by the solvent polarity effect.[43] In view of said facts, we carried out steady state fluorescence emission measurements to investigate the probability of the intramolecular proton transfer process in the excited state (ESIPT) in the case of azo derivative **2**. The azo derivatives studied here are weakly fluorescent. This may arise probably due to the electron transfer fluorescence quenching by the lone pair of electron present on the nitrogen atom of the chromophoric azo subunit. Figure S10 shows the excitation and emission spectra for **2**. The fluorescence excitation spectra in ACN/H_2O (1:1) at the detection wavelengths 435, 425, 560, and 570 nm have not revealed any reproducible and characteristic absorption spectrum of **2**, i.e., a strong absorption maximum at around 435−478 nm. When **2** was subjected to excitation at 474 nm, a weak emission band at 570 nm was observed; however, the fluorescence excitation spectrum at the detection wavelength 570 nm was able to reproduce, up to some extent, the characteristic absorption spectrum, and a red-shift was also observed. The red-shifted excitation band in 440−500 nm range may be responsible for the enol emission exclusively.[40f] Thus, the experimental observations have suggested about the less possibility of emission from a single emitting moiety, consequently the less probability for ESIPT process in the studied azo-phenol system. The photoirradiation studies carried out to establish the cis−trans (Z, E) isomerism show the disappearance of absorption maxima corresponding to the hydrazone form, and the large Stoke's shift including low quantum yield in the case of derivative **2** all together have envisaged about the photoinduced proton transfer process.

Solvatochromism and Effect of Micellar Medium. Among the derivatives **2**−**5**, we found that derivative **2** somehow differs in its characteristic optical properties and we considered it as a typical example for further studies. Since **2** has demonstrated variation in its optical signals in different media, we carefully examined the absorption and emission spectra in different nonpolar, aprotic and protic polar solvent systems, gradient systems, and also in cationic, anionic and neutral micellar systems. The absorption spectra (Table S1 and Figure S11, Supporting Information) in benzene and dichloromethane have revealed low energy bands at 482 nm ($\varepsilon = 26\,300$ $M^{-1}cm^{-1}$) and 478 nm ($\varepsilon = 24\,250$ M^{-1} cm^{-1}) while the high energy bands appeared at 333 and 327 nm, respectively. In polar-aprotic solvents such as acetonitrile (ACN) and tetrahydrofuran (THF), the low energy bands were blue-shifted for 6−10 nm to appear at 472 nm ($\varepsilon_{(ACN)} = 25\,550$ M^{-1} cm^{-1} and $\varepsilon_{(THF)} = 26\,400$ M^{-1} cm^{-1}). When **2** was subjected to more aprotic polar mediums, such as, 1,4-dioxane and DMSO, the low energy band has illustrated, abruptly red shift and appeared at 575 nm ($\varepsilon_{(dioxane)} = 21\,600$ M^{-1} cm^{-1}) and 586 nm ($\varepsilon_{(DMSO)} = 36\,550$ M^{-1} cm^{-1}), whereas the high energy bands were further blue-shifted for ∼5−10 nm to appear at 329 and 323 nm, respectively. Contrary, in polar protic solvents, such as in methanol and water, the absorption bands were significantly blue-shifted to appear at $\lambda_{max} = 466$ ($\varepsilon_{(MeOH)} = 25\,450$ M^{-1} cm^{-1}), 327 and 468 ($\varepsilon_{(water)} = 13\,800$ M^{-1} cm^{-1}), 326 nm, respectively, and ε value was found minimum in water. The absorption spectrum of **2** in 1:1 gradients of ACN−water, MeOH−water, and dioxane-water mixed solvent systems illustrate high energy bands at $\lambda_{max} = 474$ ($\varepsilon_{(ACN-water)} = 24\,000$ M^{-1} cm^{-1}) and 470 ($\varepsilon_{(MeOH-water)} = 17\,550$ M^{-1} cm^{-1}) and at $\lambda_{max} = 582$ ($\varepsilon_{(dioxane-water)} = 20\,350$ M^{-1} cm^{-1}), 483, and 331 nm, respectively. Upon increasing the water percentage the ε value corresponding to low energy band decreases and was found to be optimum for ACN−water mixed solvent system in 1:3 ratio (at $\lambda_{max} = 472$ nm; $\varepsilon_{(ACN-water)} = 16\,150$ M^{-1} cm^{-1}). Moreover, the color of solutions in different solvent systems was changed as depicted in Figure S11 (Supporting Information).

The compound **2** when excited at low energy band have revealed weak fluorescence in different solvent systems with Stoke's shift of 71−101 nm; however, when **2** was subjected to excitation at $\lambda_{max} = 334$ nm corresponding to the azo chromophore, a relatively enhanced fluorescence was observed in non polar solvent like benzene and in dichloromethane and in ACN/H_2O (1:1) gradient system with Stoke's shift in the range of 51−144 nm, respectively (Table S1, Supporting Information).

In order to observe the optical behavior in micellar mediums, we selected cetyltrimethyl ammonium bromide (CTAB), sodium dodecyl sulfate (SDS), and Triton X-100 (TX-100) surfactants as a typical representative for cationic, anionic, and neutral micellar medium and monitored both the absorption and emission after the addition of different concentrations of each individual surfactants to the solution of **2** in ACN/H_2O (1:1)

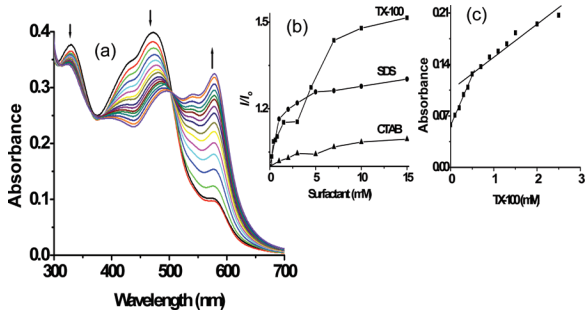

Figure 4. (a) Changes in the absorption spectrum of **2** upon addition of Triton X-100. Inset (b) Change in fluorescence intensity signal in the presence of surfactants (♦)Triton X-100, (■) SDS, and (▲) CTAB and (b) critical micellar concentration in TX-100.

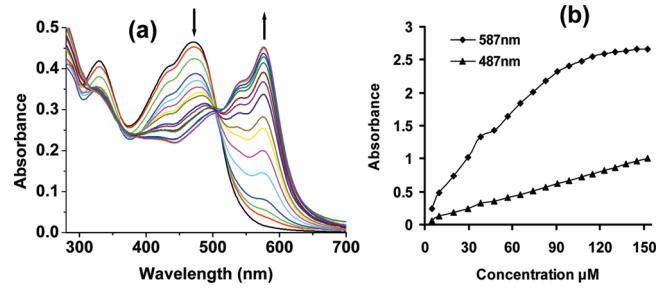

Figure 5. (a) Absorption spectra of **2** ($c = 2 \times 10^{-5}$ M) in DMSO/ACN mixed solvent system. The concentration of DMSO was increased stepwise to the solution of **2** in acetonitrile. (b) The nonlinear calibration curve obtained by increasing the concentration of **2** in DMSO solution and change in optical density at two wavelengths.

mixed solvent system. The absorption spectra have not shown any significant modulation in the CTAB and SDS (0−17 mM) micellar systems (Figure S12, Supporting Information). However, the absorption spectra in the presence of neutral micellar medium (Triton TX - 100) have illustrated significant modulation and were found to be almost similar to the aprotic polar solvent systems (Figure 4a) in which the low energy band centered at 474 nm wavelength was gradually reduced by the increase in the concentration of triton to the solution of **2**, and concomitantly, a new band toward the higher wavelength region (at $\lambda_{max} = 577$ nm) was developed with a clear isosbestic point at 506 nm wavelength.

Similarly, the emission spectra of **2** after the stepwise addition of different concentration of TX-100 have illustrated (Figure 4b) a considerable enhancement in the emission intensity at 434 nm, when subjected to an excitation wavelength at 354 nm. The critical micellar concentration, 0.5 mM for TX-100 with respect to **2** in ACN/H_2O (1:1) gradient system, was estimated[44] by ratiometric calculation of fluorescence data (Figure 4c). Figure 4b shows that after the addition of 0.5 mM of the concentration of triton fluorescence spectrum of **2** was gradually increased. Thus, the alterations in the photophysical behavior of **2** in various solvent systems encouraged us to hypothesize about the existence of equilibrium between ionized and un-ionized species, as projected in eq 3 favorably as a consequence of solvatochromism.[45] The similar effect observed in case of micellar medium can also be accounted for either ionization of **2** or interaction with hydrophilic polyethylene oxide units of nonionic surfactant (TX-100).

In general, effects such as inter and intramolecular hydrogen bonding, solvent basicity, polarizability, dispersive forces, electrostatic forces, and proton-solvent interactions play vital role in the ionization process of a molecule of low pK_a value[46] (relatively more acidic nature). We try to estimate the pK_a value for studied azo derivatives **2**, **4**, **5**, and **6** in ACN/H_2O (1:1) solvent system (Figure S13). Because of the existence of azo-hydrazone tautomers in the equilibrium, the approximate pK_a value of 9.0 ± 0.3 for unsubstituted derivative **4** was found to be relatively higher than those for **2**, **5**, and **6** which was in the range of 6.9−8.1 ± 0.3, therefore, suggesting the weak basic character for all of the studied derivatives, in which the $-NO_2$ substituted derivative **2** was of relatively more acidic character. The absorption spectra of **2** have illustrated a red-shift in the polar aprotic solvents such as DMSO and dioxane and a small red-shift in the solvents of relatively low polarity such as benzene, dichloromethane, and acetonitrile and to some extent in polar protic solvent like methanol. The dominance of the hydrazone form in the case of **2** in benzene solution is possibly due to the larger polarizability and quadrapole moment of benzene (dipole moment = 0.0; polarizability/volume = 0.070; quadrapole moment 3.6×10^{-26} $erg^{1/2}$ $cm^{5/2}$).[39d] Benzene itself has some weak Lewis basicity, which would stabilize the azo form, however, since the dipole-quadrapole and dipole−induced dipole forces[39d] of benzene dominates, therefore, the weak basicity factor apparently play little effect and molecule in benzene solution dominantly exist in the hydrazone form. Consistently, the dominance of hydrazone tautomer in equilibrium in the case of dichloromethane can be accounted by considering the little more basicity and hydrogen bond donating ability.[39d]

Likewise the anticipated significant red-shift observed in the polar aprotic solvent can also be rationalized by considering certain parameters, such as the possibility of intermolecular hydrogen bonding, degree and kind of structuring of the solvent, and the manner in which this structuring influences the salvation of azo-phenol derivatives, **2**, in which the oxygen atom is surrounded by neighboring hydrogen and/or hydrogen bond accepting ability of polar aprotic solvent such as DMSO (high basic character and low ionization potential) and/or by assuming an intermolecular charge transfer transition.[39c,e] This CT transition involves an electron transfer from the lone pair of electrons available with polar aprotic solvents to the antibonding orbital of the solute, such as −OH bond of the naphthol moiety in case of derivative **2.** Additionally, the high electron accepting property of nitro substituent present on the BT unit would also reflect weakening of the O−H bond as a result of the decreased electron density on the oxygen atom.

To establish the CT transition in the case of azo derivative **2**, a nonlinear fitting relationship, between the absorption band at 487 nm and a new band generated at 587 nm wavelengths corresponding to the different molar concentration of compound **2** was obtained. Figure 5b shows a linear increase in the absorbance of 487 nm band as the concentration of **2** in DMSO solution was increased from 5 to 153 μM; however, the new band appearing at 587 nm shows a nonlinear behavior. Thus, suggesting about the intermolecular CT character and that would be originated from the naphthol unit, toward the high electron accepting BT unit.[39f−i] Moreover, in order to investigate the possibility of aggregation/complexation, another experiment was performed by increasing the molar concentration of DMSO solution from 0.64 to 10.24 mmol to the solution of **2** ($c = 2 \times 10^{-5}$ M) in acetonitrile (Figure 5a). The formation of an isosbestic point at ∼506−10 nm, in which the absorption band appeared at 472 nm, was gradually decreased and concomitantly a new band appeared at 577 nm, and also the color of solution changed from a light yellow orange to purple blue, have clearly suggested the possibility for the formation of a solvated complex with **2** and therefore indicating the establishment of an equi-

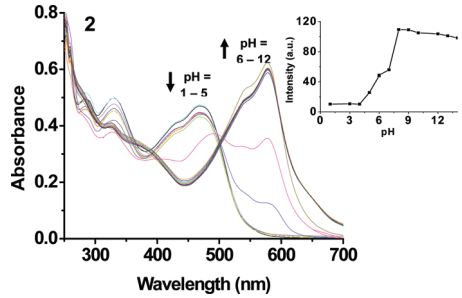

Figure 6. Change in the absorption and emission band (inset) of **2** under different pH conditions.

librium between the free and H-bond solvated species in the medium. The red-shift observed in the absorption spectrum of **2** in dioxane solution upon the addition of water was gradually reduced and similarly, the absorption spectrum of **2** was regenerated upon increasing the percentage of water molecule to the solution of **2** in DMSO. Since a water molecule has a greater tendency to donate hydrogen bond than any other solvent molecules,[46] the conjugate base (ionized species, A^-) formed in the medium will be destabilized by hydrogen-bonding interaction, thus deserting the chance of intermolecular hydrogen bonding with aprotic polar solvent and Triton X-100.

$$\mathbf{HA} \rightleftharpoons \overset{\oplus}{\mathbf{H}} + \overset{\ominus}{\mathbf{A}} \qquad (3)$$

To affirm above hypothesis acid−base titration experiment was performed. The absorbance spectra with respect to different pHs (Figure 6) in ACN/water solvent mixture revealed that **2** predominantly exist in the hydrazone form in the acidic medium, between pH 1 and 6. To maintain the particular pH in the medium for **2** and other derivatives a B/BH^+ buffer was attained in ACN/H_2O solvent system as mentioned in the experimental section. As the pH of the medium was moved up the characteristic absorption maxima at 474 nm was gradually reduced and a new band was appeared at ∼585 nm between pH 7 and 7.5 and, become dominant after pH 8 and onward with substantially high molar absorptivity. A red-shift of ∼110−115 nm with an isosbestic point at 496 nm was observed which clearly suggested about the existence of two species (un-ionized and ionized) in the medium as a result of deprotonation of hydroxyl proton. Similarly, the acid−base titration studies with derivatives **5** and **6** containing electron donating substituents $-CH_3$ and $-OCH_3$ on BT unit consistently undergo ionization reaction between pH 6 and 12, and a new broad band at higher wavelength, ∼553−558 nm, appeared in both the cases (Figure S14).

According to de Silva et al.,[47] the enhancement in the emission intensity is attributable to restricted photoinduced electron transfer reaction (PET). Reversely, the enhanced PET reaction may be one of the reasons for fluorescence quenching under the condition. To observe that, pH-emission spectra for **2** and other derivatives **4**−**6** have been analyzed by exciting the derivatives at their respective excitation wavelengths. The pH-emission spectra of **2** in the pH range 1−5 have illustrated a marginal enhancement in the emission intensity, which upon increasing the OH^- concentration in the medium, around pH 6−8 was abruptly enhanced and almost become constant in between pH 8 and 12. Consistently, the pH-emission spectra of other derivatives have also shown similar changes in the emission band with respect to the different pHs. The red-shift encountered in the absorption spectra in the alkaline medium and enhancement in the emission intensity have clearly suggested the ionization reaction in the medium. Consequently, with the formation of deprotonated anionic species, the electron density around the chromophoric azo unit increases, which would lead to the increase in electron delocalization. Additionally, the delocalized π-conjugated bond will be of higher energy and would result in a red shift in the absorption spectra and significant enhancement in the fluorescence intensity. Moreover, the marginal rise in the emission intensity in the pH range 1−5 could be reasoned for the protonation of one of the nitrogen atom of azo chromophore (Scheme 3) and was evidenced by the regeneration of both the absorption and emission bands upon increasing the H^+ concentration in the medium. Thus, the pH studies clearly demonstrate the existence of **2** in the equilibrium of ionized and un-ionized forms and also the feasibility of receptor to work as a sensor under physiological pH conditions.

Metal−Ion Interaction Studies. The metal ion binding affinity of **2**, **3**, **4**, and **5** have been monitored by absorption and emission spectra in aqueous-acetonitrile (CH_3CN/H_2O; 1:1) mixed solution. Upon the addition of different metal ions (5 equiv) such as, Na^+, K^+, Ca^{2+}, Ag^+, Co^{2+}, Ni^{2+}, Zn^{2+}, Cd^{2+}, Hg^{2+} and Cu^{2+} to solutions of receptors **2**, **3**, **4** and **5** separately, characteristic color changes in the solutions were observed, (Figure 7) and the absorption spectrum of **2** was modulated selectively by both Hg^{2+} and Cu^{2+} metal ions, in which the low energy charge transfer band centered at 474 nm was completely disappeared and instantaneously, two new absorption maxima were appeared at 550 and 588 nm and one at 585 nm

SCHEME 3: Protonation and Deprotonation Behavior of Azo-Phenol Derivatives

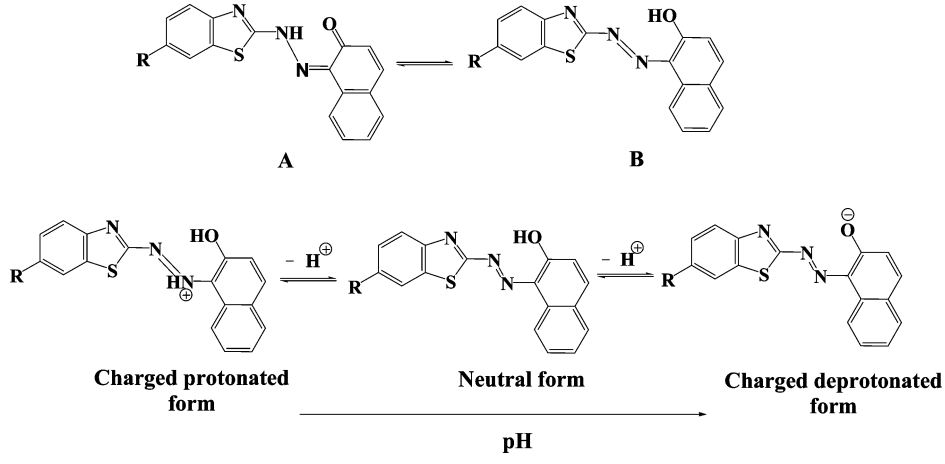

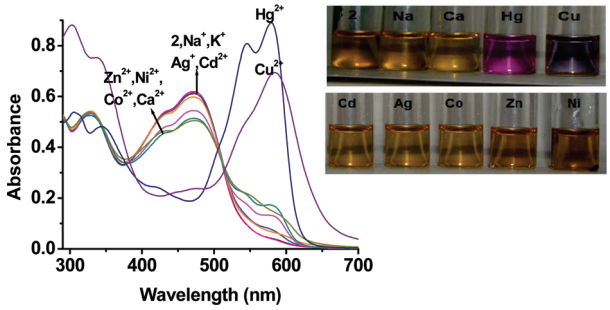

Figure 7. Chnge in absorption spectra of **2**, upon intercation with different metal ions. Inset: Photographs illustrate the change in color of **2** in the presence of different metal ions.

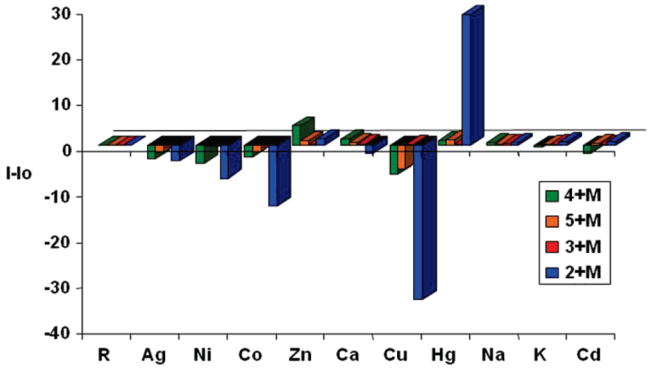

Figure 8. Barr graph shows comparative fluorescence intensity for receptors **2**−**5** in THE presence of different metal ions.

in case of Cu^{2+} ion respectively. Likewise, the high energy band, centered at 332 nm was completely disappeared and/or exhibited a red shift for ∼24−28 nm upon interaction with both Hg^{2+} and Cu^{2+} metal ions. Interestingly, the color of the solution in the presence of Hg^{2+} and Cu^{2+} ions was changed from a yellow-orange to pink and blue-gray respectively (Figure 7, inset). The other metal ions have not been able to induce any significant change in the absorption spectrum of **2**, except for a little hypochromism in the presence of Zn^{2+}, Ni^{2+}, Co^{2+}, and Ca^{2+} metal ions. Similarly, when other derivatives **3**−**5** were treated with different metal ions, **4** and **5** have shown (Figure S15 and S16, Supporting Information) changes in the absorption spectra and color in the receptor solutions but not selectively and specifically. Receptor **5** has shown the greater affinity for Hg, Cu, Co, Ni, Zn, and Cd transition metal ions in which the low energy band of absorption spectra attributed to the hydrazone-azo tautomers was completely disappeared and a new band was appeared in the longer wavelength region. The variation in molar extinction coefficients were found in the order of $\varepsilon_{Cu^{2+}} > \varepsilon_{Hg^{2+}} > \varepsilon_{Co^{2+}} > \varepsilon_{Zn^{2+}} > \varepsilon_{Ni^{2+}} > \varepsilon_{Cd^{2+}}$. The absorption spectrum of **3** was remained unchanged (Figure S17, Supporting Information).

The fluorogenic behaviors of **2**, **4** and **5** (10 μM) have been investigated separately by measuring the emission spectra, at 354 nm excitation wavelength, by the addition of tested metal ions (50 equiv) to the respective solutions in CH_3CN/H_2O (1:1 *v*/*v*). The relative change in the fluorescence intensities corresponding to the different metal ions have been represented with the help of a bar graph, which shows (Figure 8) that the receptors **4** and **5** have not been able to induce any significant change in the emission band; however, the emission spectrum of **2** was considerably modulated in which the fluorescence intensity signal, at 447 nm, was significantly enhanced and quenched in the presence of Hg^{2+} and Cu^{2+} metal ions, respectively (Figure 9). The fluorescence intensity in the presence of different metal ions was estimated and found in the following order: Na^+ (1.4%), K^+ (1.8%), Cd^{2+} (1.9%), Zn^{2+} (3.1%), Hg^{2+} (62.2%), Ca^{2+} (−3.7%), Ag^+ (−7.4%), Ni^{2+} (−15.7%), Co^{2+} (−29.0%), and Cu^{2+} (−80.0%). The data clearly indicated the higher selectivity of **2** for Hg^{2+} and Cu^{2+} ions among the tested metal ions in which ∼62% enhancement and ∼80% quenching in the relative fluorescence intensity was observed, respectively. Additionally, the color of solution under UV light changed from a fluorescence blue to green and light brown for Hg^{2+} and Cu^{2+} ions, respectively (Figure 9, inset). Thus, the metal ion interaction studies are in support of **2** to act as an aqueous medium compatible chromo and fluorogenic sensor for both Hg^{2+} and Cu^{2+} metal ions. Also, in the prospect of obtaining better optical signals, the considerable change observed in the absorption and emission intensity signals signifies the utility of polar effect exerted by appended $-NO_2$ substituent in **2** among the synthesized derivatives. The quantum yield estimation[48] for **2** has been carried out in acetonitrile solution with respect to naphthalene ($\phi_{NP} = 0.2$) using secondary method ($Q = Q_R(I/I_R)(OD_R/OD)(n^2/n_R^2)$, where Q is the quantum yield, I is the integrated intensity, OD is the optical density, and n is the refractive index and the subscript R refers to the reference fluorophore of known quantum yield) and was found to be $\phi_2 = 0.038$. The enhancement in quantum yield (∼1.4 times) of **2** upon interaction with Hg^{2+} metal ion ($\phi_{2+Hg^{2+}} = 0.054$), and quenching in the fluorescence quantum yield (∼7.6 times) with Cu^{2+} metal ion ($\phi_{2+Cu^{2+}} = 0.005$) have further supported about relatively more selectivity of **2** for Hg^{2+} metal ion.

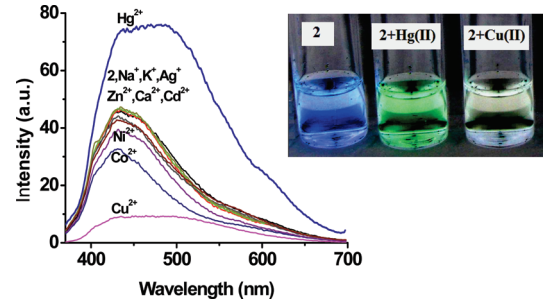

Figure 9. Fluorescence spectra for **2**, upon intercation with different metal ions. Inset: Photographs showing the change in color under UV light (365 nm).

UV−Vis and Fluorescence Titration Studies with Hg^{2+} and Cu^{2+} Metal Ions. The affinity and sensitivity of chemosensor **2** for both Hg^{2+} and Cu^{2+} ions has been further monitored by the absorption and fluorescence titration experiment studies in aqueous-acetonitrile solution. Upon increasing the concentration of Hg^{2+} ion ($c = 2.5 \times 10^{-3}$ M, 3 μL = 0.15 equiv; in CH_3CN/H_2O; 1:1; *v*/*v*) to the solution of **2** ($c = 2 \times 10^{-5}$ M, CH_3CN/H_2O), the low energy charge transfer band centered at 474 nm was gradually reduced and concomitantly, two new bands toward the longer wavelength region were appeared at 550 and 588 nm (Figure 10a). It was interesting to observe that after the addition of 1.2 equiv of Hg^{2+} ion the high energy band at 331 nm was gradually reduced and a new band at 307 nm appeared. On further increase in the concentration of Hg^{2+} ion (3 equiv), absorption spectra reached saturation concurrently; the characteristic bands of receptor **2** were completely disappeared. The two well-defined isosbestic points observed at 391 and 512 nm have clearly suggested the existence of a unique complex in the medium along with the free ligand. Further, the characteristic change observed in the absorption spectrum of **2** in the presence of Hg^{2+} ion has indicated the involvement of a complexation reaction between **2** and a mercury ion, as a consequence of possible change in the geometric configuration

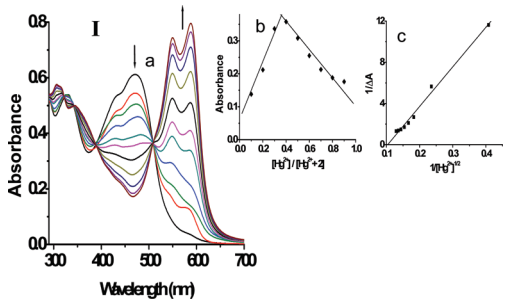

Figure 10. (I) UV−vis absorption titration spectra of chemosensor **2** ($c = 2 \times 10^{-5}$ M) on addition of Hg^{2+} ion in aqueous-acetonitrile solution. Insets: Shows (b) Job's plot for 2:1 stoichiometry and (c) a straight line for B−H plots upon interaction of **2** with Hg^{2+} metal ion in ACN/H_2O (1:1; *v*/*v*) mixed solvent system.

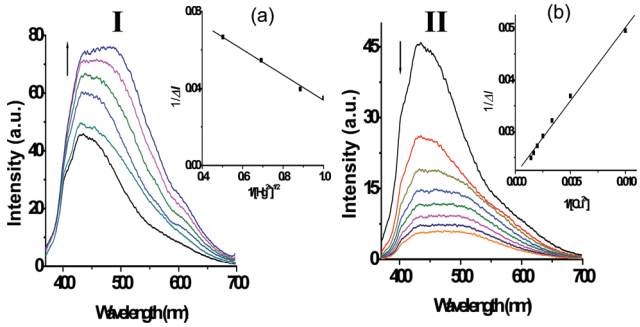

Figure 11. Fluorescence titration spectra of chemosensor **2** ($c = 1 \times 10^{-5}$ M) on addition of Hg^{2+} (I) and Cu^{2+} (II) ions in aqueous-acetonitrile solution. Insets (a) and (b) shows B−H plots.

of **2** from trans to cis. The change in the color of solution from a yellow-orange to a pink favors **2** for visible "naked-eye" detection of Hg^{2+} ion. A 2:1 stoichiometry has been realized by Job's plot analysis.[49] The association constant for 2:1 stoichiometry (Figure 10b) has been calculated by B−H equation[50] (4) from the non linear fitting of absorption titration curves and found, $K_{assoc} = 1.04 \pm 0.3 \times 10^5$ M^{-2} that further suggested about the ML_2 type of complexation[51] between **2** and Hg^{2+} ion through the probable potential donor sites (Figure 10c).

$$1/(I - I_0) = 1/(I - I_f) + 1/K(I - I_f)[M]^{1/2} \quad (4)$$

$$1/(I - I_0) = 1/(I - I_f) + 1/K(I - I_f)[M] \quad (5)$$

In the fluorescence titration experiment, receptor **2** was subjected to excitation wavelength at 354 nm and was monitored after each stepwise addition of Hg^{2+} ion to the solution of **2**. A gradual enhancement (~62%) in the fluorescence intensity was observed, at 447 nm emission band, upon increasing the concentration of Hg^{2+} ions (~50 equiv; Figure 11, I) that could be assigned to complexation reaction between **2** and Hg^{2+} ion as a result of deprotonation of hydroxyl function, and involvement of N, O, and S atoms in coordination. Consequently, the fluorescent blue color of sensor solution was changed to light green under the UV light (Figure 9, inset). The 2:1 stoichiometry was further realized by the Job's plot analysis, and an association constant for 2:1 stoichiometry using eq 4 was estimated by nonlinear fitting of fluorescence titration curves. A straight line obtained (Figure 11, Ia) for B−H plot with $K_{assoc} = 1.51 \times 10^5$ $/M^2$ has confirmed the extent of complexation between **2** and Hg^{2+} metal ion.

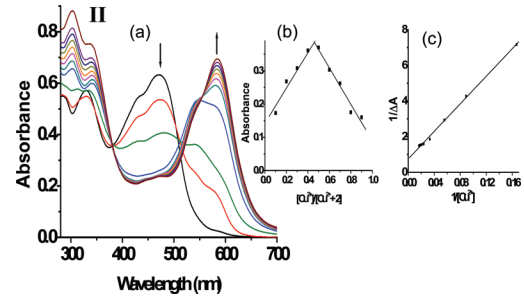

Figure 12. UV−vis absorption titration spectra of chemosensor **2** ($c = 2 \times 10^{-5}$ M) on addition of Cu^{2+} (II) ions in aqueous-acetonitrile solution. Insets: (b) Job's plot and (c) B−H plot.

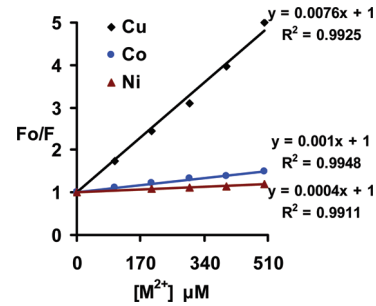

Figure 13. S−V plot for **2** in the presence of M^{2+} (Cu(II), Co(II), and Ni(II)) ions.

Similarly, to understand the binding affinity and sensitivity of **2** for Cu^{2+} metal ion, equivalents of copper nitrate ($c = 2.5 \times 10^{-3}$ M, 3 μL = 0.15 equiv) in CH_3CN/H_2O were added to the solution of **2** ($c = 2 \times 10^{-5}$ M). The absorption spectra (Figure 12a) have shown rapid (after the addition of 0.3 to 0.6 equiv of Cu^{2+} ion) modulation, in which the low energy band completely disappeared after the addition of 2 equiv of Cu^{2+} ion. Concurrently, the high energy bands were rationalized, and a new band appeared at 585 nm. The formation of clear isosbestic points at 383 and 557 nm have suggested about the change in geometrical configuration of **2** from trans to cis and also about the existence of a unique complex along with free receptor in the medium. The Jobs' plot analysis (Figure 12b) has revealed a 1:1 stoichiometry for probable complexation reaction between **2** and Cu^{2+} metal ion. A straight line for B−H plot (figure 12c) with an association constant, $K_{assoc} = 0.193 \times 10^5$ M^{-1} was obtained through the eq 5 by utilizing nonlinear fitting of absorption titration curves, which has further supported the stoichiometry for complexation reaction.

The fluorescence titration spectra of chemosensor **2** under similar experimental condition have demonstrated a gradual decrease in the fluorescence intensity. Upon increasing the concentration of Cu^{2+} ion to the solution of **2** the emission band centered at 447 nm wavelength was quenched by ~87% (Figure 11, II). For a quantitative measurement of fluorescence quenching Stern−Volmer (S−V) plot was obtained between Fo/F and Cu^{2+} ion concentration (Figure 13). A linear S−V plot ($R^2 = 0.9925$) with quenching constant $K_{sv} = 7600$ M^{-1} has clearly suggested the dynamic mode of quenching for paramagnetic Cu^{2+} metal ion and can be attributed to the metal to ligand charge transfer (MLCT) reaction. The weak association constant, $K_{assoc} = 0.08 \times 10^5$ M^{-1}, calculated by nonlinear fitting of fluorescence titration curves is itself explain about the strength of complexation between **2** and Cu^{2+} metal ion. Both the Co^{2+} and Ni^{2+} ions were not able to illustrate any significant change in the absorption spectrum of **2**; however, they have shown relatively weaker fluorogenic affinity, as envisaged by association constants 1.21 and 0.82 of the log *K* value, respectively.

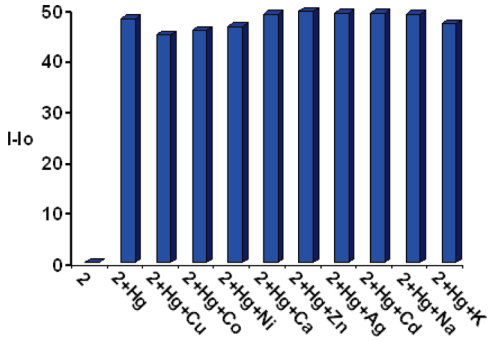

Figure 14. Bar graph showing interference study of receptor **2** (2×10^{-5} M), $2+Hg^{2+}$ and $2+Hg^{2+}$ + M ions.

Metal Ion Selectivity. In order to understand the selectivity of **2** with Hg^{2+} or Cu^{2+} and/or other tested metal ions, an interference study has been carried out by the addition of different metal ions (5 equiv) to the solution of **2** in a particular order. First, Hg^{2+} ion was added and both the absorption and emission spectra were measured then rest of tested metal ions, including Cu^{2+} ion were added. Reversely, first Cu^{2+} and other metal ions followed by Hg^{2+} ion were added to the solution of **2** and both absorption and emission spectra were monitored. Interestingly, the change in the absorption and emission spectra at their respective bands were found to be almost identical (±3−7% SD) to the corresponding bands of **2** + Hg^{2+} metal ion complex (Figure 14). Thus, azo-phenol derivative **2** having nitro substituent at C-6 of benzothiazolyl ring, was found as a naked-eye sensitive chemosensor that can selectively detect the Hg^{2+} ion in the aqueous−organic medium by the characteristic changes in their chromo and fluorogenic optical properties.

FT-IR Analysis. The probable complexation reaction between **2** and Hg^{2+} ion was further observed by detailed FT-IR spectral analysis in the range of 4000−400 cm^{-1} (Figure S18, Supporting Information). The IR spectrum of **2** illustrates the stretching vibration bands at 3431, 1622, 1572, 1522, 1446, 1335, and 677 (weak band) cm^{-1} probably, corresponding to the azo/hydrazo, υ(NH/OH), υ(C═N) for nitro group and of thiazole ring, and υ(N═N) for azo chromophore respectively. The bands that appeared at 1280, 832, and 754 cm^{-1} can be assigned to C−H stretching vibrations of aromatic region. The characteristic stretching vibrations in FT-IR spectrum favors the existence of **2** predominantly in the hydrazone form.[52] Upon **2** + Hg^{2+} ion complexation, by the addition of 5 equiv of mercury to the solution of **2**, the respective stretching vibration bands were either reduced and/or shifted (6−20 cm^{-1}) toward the lower frequency region (Figure S19). Moreover, upon interaction with Hg^{2+} ion the probable OH/NH stretching vibration band at 3431 cm^{-1} was reduced or disappeared, and concomitantly a new characteristic band at 1089 cm^{-1} that could be attributed to strong M−O interaction appeared. The vibration bands, probably assigned for the C−O stretching vibrations at 1280, 1170, and 1125 cm^{-1} after the addition of Hg^{2+} ion, have also illustrated considerable blue-shift for 191−36 cm^{-1}. Further, a weak vibration band at 479 cm^{-1} upon treatment with Hg^{2+} ion was regenerated strongly and that can be possible by a strong M-N (metal to nitrogen) interactions. Therefore, the characteristic changes in the FTIR spectra have suggested the probability of complexation between **2** and Hg^{2+} ion by the hypothesized coordination sites, in the form of N and O atoms, that could be possible only by the removal of a probable azo/hydrazo tautomeric proton.[53] Similarly, the FTIR spectrum of **2** with Cu^{2+} ion have illustrated more or less same type of interaction for complexation (Figure S20).

SCHEME 4: Proposed Mechanism for Complexation of 2 with Hg^{2+} and Cu^{2+} Metal Ions in ACN/H_2O (1:1) Solvent System

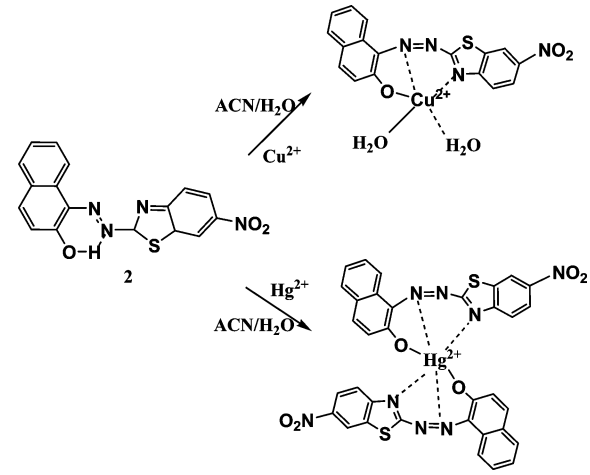

To verify the binding sites in **2** with Hg^{2+}/Cu^{2+}, azo derivative **3** as a control molecule was synthesized. Under similar experimental conditions, the absorbance of **3** does not show any significant modulation or shift after the addition of Hg^{2+} ions (Figure S17). The vibration band corresponding to OH/NH function completely disappeared. The FT-IR spectrum of **3** (Figure S21) only shows characteristic vibration bands at 1095, 1028, 1438, and 680 cm^{-1} that can be attributed to C−O−C, −N═N−, and C−S stretching vibrations, respectively. After treating **3** with Hg^{2+} ion, the vibration band corresponding to the azo band at 1458 cm^{-1} was reduced while other bands merged together and became broadened (Figure S22), thereby clearly supporting the interaction of Hg^{2+} metal ion with azo chromophoric unit also. On the basis of the above experimental evidence, we proposed that **2** would favorably coordinate with metal ions by the phenolic oxygen atom, the azo nitrogen atom adjacent to the naphthol ring, and the thiazole nitrogen of benzothiazole ring in a terdentate manner leading to the formation of five-membered chelate ring.[53] The change in the photophysical properties of **2** both in the absence or presence of metal ions and relatively strong complexation between **2** and Hg^{2+}/Cu^{2+} in 2:1/1:1 stoichiometry, respectively, can be easily understood by assuming **2** as a planar terdentate molecule[53] and by assuming that the resulting **2** + Cu^{2+} and **2** + Hg^{2+} complexes would be able to attain either a distorted square pyramidal[54] and/or octahedral structure,[55] respectively, in the medium, as depicted in Scheme 4. The proposed mode of interaction with both the metal ions would be nearly close to that observed in the crystals of different complexes reported by Kurahashi et al.[56]

^{1}H NMR Titration Study. To arrive at an actual mechanism involved for "naked-eye" visual color change in sensing event, a ^{1}H NMR titration experiment was performed in $CDCl_3$ for **2** ($c = 1.14 \times 10^{-2}$ M). The downfield shift observed for the hydrazone proton is presumably due to hydrogen bonding interaction with azo chromophore via a predicted six-member cyclic transition state and/or also due to the interaction with $\pi-el^-$ cloud of geometrically trans aromatic rings. The ^{1}H NMR titration spectra (Figure 15), after the addition of 0.3 equiv (= 6 μL) of Hg^{2+} ion (as perchlorate salt, in CD_3CN, $c = 2.8 \times 10^{-1}$ M) show a narrow downfield shift for the protons of the benzothiazole ring. On increasing the concentration of Hg^{2+} ions (0.6 equiv; Figure S23), the resonance signal attributed to *N−H* proton have shown downfield shift (δ 15.803) and

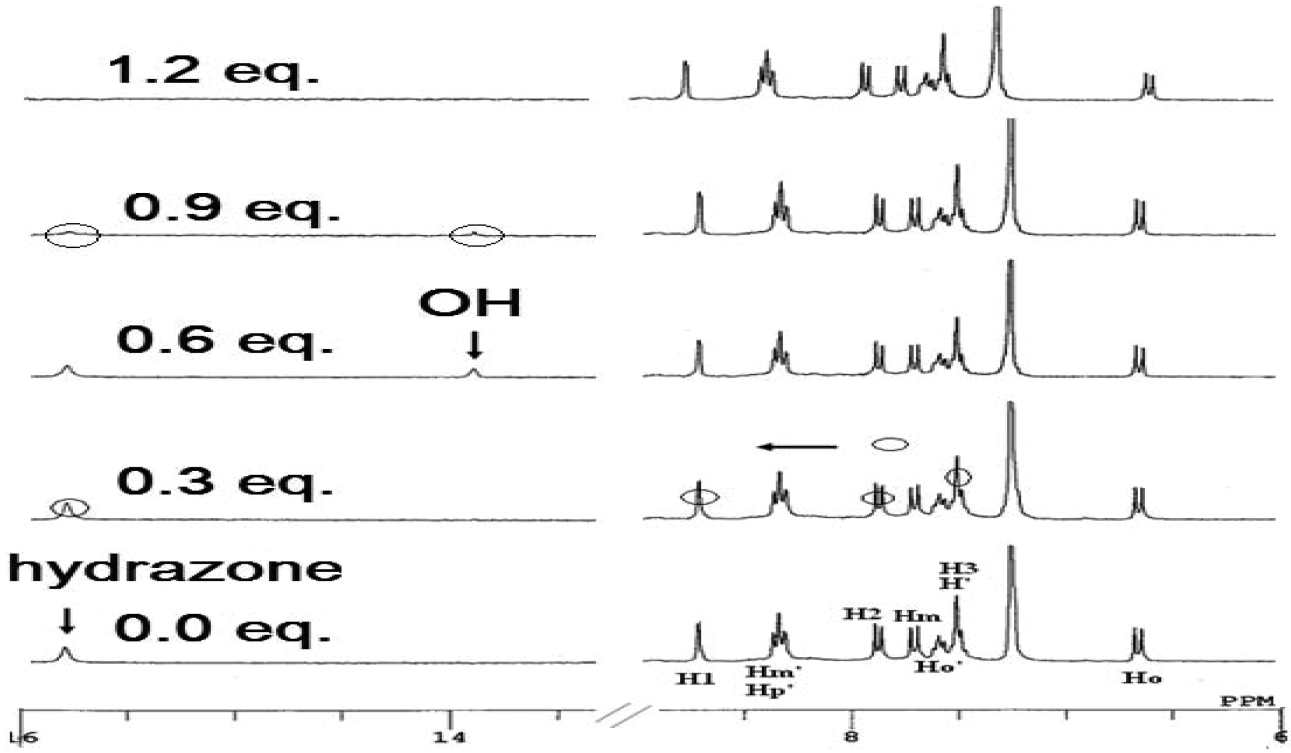

Figure 15. ^1H NMR titration spectra in $CDCl_3$ for chemosensor **2** upon addition of different equivalents of Hg^{2+} ion as $Hg(ClO_4)_2$.

simultaneously, a new signal probably as a result of formation of a tautomeric phenolic form in the solution, was appeared at δ 13.909. As predicted, the resonance signals for *O*−*H* and *N*−*H* (of hydrazone) protons after addition of Hg^{2+} ions (0.9 equiv) were further reduced along with their respective chemical shifts and were completely disappeared after addition of 1.2 equiv of Hg^{2+} ions. In addition, the significant low-field shift ($\Delta\delta = 0.017$) for H1 proton of benzothiazole unit could be reasoned to a decrease in electron density, because of involvement of N-atom of benzothiazole unit in the complexation. The ^1H NMR spectral analysis as discussed thus, clearly suggested about the generation of phenolic derivative by a proton transfer reaction in an early transition state of metal ion sensing event and, complexation was attained later on by complete deprotonation of phenolic proton. Moreover, to justify the predicted downfield shift for *N*−*H* and/or *O*−*H* proton, the sample solution was treated with D_2O. The corresponding signals, observed at δ 15.796 (*N*−*H*) and at δ 13.91 (*O*−*H*) were disappeared (figure S24) henceforth, it is made clear that, in the **2**-Hg^{2+} system, *N* atom of azo chromophore, and of benzothiazole ring and *O* atom of naphthol ring are involved in complexation.

Detection of Hg^{2+} Ion on a Cellulose Paper Strip. To demonstrate the applicability of chemosensor **2** on a paper strip, test paper strips made up of cellulose were prepared (1.5 × 0.5 cm^2) by treating the paper with a solution of **2** in dichloromethane (4 mg/mL) and dried in air. Mercury nitrate solutions of two different concentrations, 2×10^{-5} and 2×10^{-6} M, were prepared in water and the test paper strips were immersed and air-dried. Figure 16 shows the change in the color of test paper strips that clearly demonstrated the potential of **2** for the detection of the Hg^{2+} metal ion on a solid paper strip.

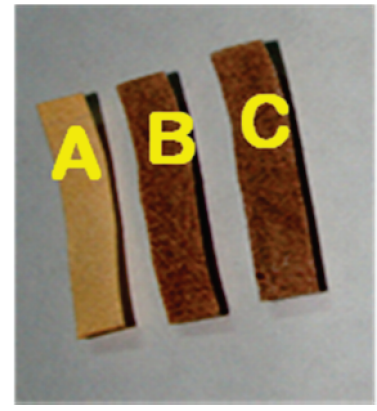

Figure 16. Changes in the color of the test paper strip prepared by adsorbing **2** on a cellulose paper film for detection of Hg^{2+} ion (A) **2** without Hg^{2+} ion; (B) **2** + Hg^{2+} (2×10^{-5}); and (C) **2** + Hg^{2+} (2×10^{-6}) in aqueous solution.

Conclusion

Conclusively, an efficient and cost-effective chemosensor has been developed that was able to detect Hg^{2+} ion selectively, in aqueous medium and on a test paper strip. The chemosensor has acted as a real time, sensitive, and naked-eye visible colorimetric sensor for Hg^{2+} ion. The ^{1}HNMR spectral analysis of derivatives **2**, **4**, **5**, and **6** have clearly indicated the existence of **2** dominantly in the hydrazone form and that it undergoes metal induced proton transfer reaction in the presence of mercury metal ion. The mode of interaction between **2** and Hg^{2+} metal ion has been further confirmed by performing similar experiments with a model compound, *N*-alkylated derivative, **3**. The absorption and FT-IR spectra of **3** have clearly supported the probability of coordination in the **2**−Hg^{2+} system, through the N atom of azo chromophore and of benzothiazole ring and O atom of naphthol ring in the terdentate fashion, possibly by attaining a distorted octahedral configuration.

Acknowledgment. We gratefully acknowledge the financial support from the Department of Science and Technology (DST), New Delhi and Council of Scientific and Industrial Research (CSIR), New Delhi for fellowship (to MS).

Supporting Information Available: UV−vis, ^{1}H NMR, ^{13}C NMR, and FT-IR spectra (Figure S1−24). This material is available free of charge via the Internet at http://pubs.acs.org.

References and Notes

(1) (a) Gunnlaugsson, T.; Glynn, M.; Tocci, G. M.; Kruger, P. E.; Pfeffer, F. M. *Coord. Chem. Rev.* **2006**, *250*, 3094. (b) Katayer, E. A.; Ustynyak, Y. A.; Sessler, J. L. *Coord. Chem.* **2006**, *250*, 3004.

(2) Nolan, E. M.; Lippard, S. J. *Chem. Rev.* **2008**, *108*, 3443.

(3) (a) Harris, H. H.; Pickering, I. J.; George, G. N. *Science* **2005**, *301*, 1203. (b) Renzoni, A.; Zino, F.; Franchi, E. *Environ. Res.* **1998**, *77*, 68. (c) Malm, O. *Environ. Res.* **1998**, *77*, 73. (d) Burg, R. V.; Greenwood, R. M. *Metals and their Compounds in the Environment*; VCH: Wienheim, Germany, 1991; pp 1045.

(4) Benit, J. M.; Fitgerald, W. F.; Damman, A. W. *Environ. Res.* **1998**, *78*, 118.

(5) (a) Boeing, D. W. *Chemosphere* **2000**, *40*, 1335. (b) Harris, H. H.; Pickering, I. J.; George, G. N. *Science* **2003**, *301*, 1203.

(6) Grandjean, P.; Weihe, P.; White, R. F.; Debes, F. *Environ. Res.* **1998**, *77*, 165.

(7) Takeuchi, T.; Morikawa, N.; Matsumoto, H.; Shiraishi, Y. *Acta Neuropathol.* **1962**, *2*, 40.

(8) Kramer, R. *Angew. Chem., Int. Ed.* **1998**, *37*, 772.

(9) Koval, I. A.; Gamez, P.; Belle, C.; Selmeczi, K.; Reedijk, J. *Chem. Soc. Rev.* **2006**, *35*, 814.

(10) Barnham, K. J.; Masters, C. L.; Bush, A. I. *Nat. Rev. Drug Discovery* **2004**, *3*, 205.

(11) (a) Sancenon, F.; Martinez-Manez, R.; Soto, J. *J. Chem. Commun.* **2001**, 2262. (b) Choi, M. J.; Kim, M. Y.; Chang, S.-K. *Chem. Commun.* **2001**, 1664. (c) Basheer, M. C.; Alex, S.; Thomas, K. G.; Suresh, C. H.; Das, S. *Tetradedron* **2006**, *62*, 605. (d) Zhu, M.; Yuan, M.; Liu, X.; Xu, J.; Lv, J.; Huang, C.; Liu, H.; Li, Y.; Wang, Su.; Zhu, D. *Org. Lett.* **2008**, *10*, 1481. (e) Huang, J.; Xu, Y.; Qian, X. *J. Org. Chem.* **2009**, *74*, 2167. (f) Pandey, S.; Ali, M.; Bishnoi, A.; Azam, A.; Pandey, S.; Chawla, H. M. *J. Fluoresc.* **2008**, *18*, 533. (g) Pandey, S.; Azam, A.; Pandey, S.; Chawla, H. M. *Org. Biomol. Chem.* **2009**, *7*, 2009. (h) Pandey, S.; Jyotsna, R.; Azam, A.; Pandey, S.; Chawla, H. M. *J. Solution Chem.* **2010**, *39*, 107.

(12) (a) Lloris, J. M.; Martinez-Manez, R.; Radilla-Tosta, M. E.; Pardo, T.; Soto, J.; Beer, P. D.; Cadman, L.; Smith, D. K. *J. Chem. Soc., Dalton Trans.* **1999**, 2359. (b) Caballero, A.; Martinez, R.; Lloveras, V.; Ratera, I.; Vidal-Gancedo, J.; Wurst, K.; Tarraga, A.; Molina, P.; Veciana, J. *J. Am. Chem. Soc.* **2005**, *127*, 15666.

(13) (a) He, G.; Zhao, Y.; He, C.; Liu, Y.; Duan, C. *Inorg. Chem.* **2008**, *47*, 5169. (b) Yuan, M.; Li, Y.; Li, J.; Li, C.; Liu, X.; Lv, Jing.; Xu, J.; Liu, H.; Wang, S.; Zhu, D. *Org. Lett.* **2007**, *9*, 2313. (c) Liu, Yu.; Han, M.; Heng-Yi Zhang, Yang, Li-Xu, Jiang, W. *Org. Lett.* **2008**, *10*, 2873. (d) Choi, M.-G.; Ryu, D.-H.; Jeon, H.-L.; Cha, S.; Cho, J.; Joo, H. H.; Hong, K. S.; Lee, C.; Ahn, S.; Chang, S.-K. *Org. Lett.* **2008**, *10*, 3717. (e) Rekha, R.; Jyothish, A. K.; Ramaiah, D. *Org. Lett.* **2007**, *9*, 121. (f) Dhir, A.; Bhalla, V.; Kumar, M. *Org. Lett.* **2008**, *10*, 4891. (g) Chen, X.; Nam, S.-W.; Jou, M. J.; Kim, Y.; Kim, S.-J.; Park, S.; Yoon, J. *Org. Lett.* **2008**, *10*, 5235.

(14) (a) Li, H.; Yan, H. *J. Phys. Chem.* **2009**, *113*, 7526. (b) Lee, J.-S.; Han, M. S.; Mirkin, C. A. *Angew. Chem., Int. Ed.* **2007**, *46*, 4093.

(15) (a) Huang, J.; Xu, Y.; Qian, X. *J. Org. Chem.* **2009**, *74*, 2167. (b) Shi, W.; Ma, H. *Chem. Commun.* **2008**, *16*, 1856. (c) Wu, J.; Hwang, I.; Kim, K.; Kim, J. *Org. Lett.* **2007**, *9*, 907. (d) Zhang, X.; Xiao, Y.; Qian, X. *Angew. Chem., Int. Ed.* **2008**, *47*, 8025. (e) Suresh, M.; Shrivastav, A.; Mishra, S.; Suresh, E.; Das, A. *Org. Lett.* **2008**, *10*, 3013. (f) Zhan, X.; Qian, Z.; Zheng, H.; Su, B.; Lan, Z.; Xu, J. *Chem. Commun.* **2008**, *16*, 1859. (g) Wu, J.; Hwang, I.; Kim, K.; Kim, J. *Org. Lett.* **2007**, *9*, 907.

(16) Cheng, Y.; Zhang, M.; Yang, H.; Li, F.; Yi, T.; Huang, C. *Dyes Pigm.* **2008**, *76*, 775.

(17) Talanov, V. S.; Roper, E. D.; Buie, N. M.; Talanova, G. G. *Tetrahedron Lett.* **2007**, *48*, 8022.

(18) Young, S. *Spectrochim. Acta, Part A* **2007**, *68*, 705.

(19) Song, K. C.; Kim, M. H.; Kim, H. J.; Chang, S. K. *Tetrahedron Lett.* **2007**, *48*, 7464.

(20) Meng, X. M.; Zhu, M. Z.; Guo, Q. X. *Chin. Chem. Lett.* **2007**, *18*, 1209.

(21) Wang, H.; Chan, W. *Tetrahedron* **2007**, *63*, 8825.

(22) Mu, H.; Gong, R.; Ma, Q.; Sun, Y.; Fu, E. *Tetrahedron Lett.* **2007**, *48*, 5525.

(23) (a) Zhang, X.; Shiraishi, Y.; Hirai, T. *Tetrahedron Lett.* **2007**, *48*, 5455. (b) Chen, X.; Nam, S.-W.; Jou, M. J.; Kim, Y.; Kim, S.-J.; Park, S.; Yoon, J. *Org. Lett.* **2008**, *10*, 5235. (c) Zhou, Y.; Wang, F.; Kim, Y.; Kim, S.-J.; Yoon, J. *Org. Lett.* **2009**, *11*, 4442.

(24) Yang, H.; Zhou, Z.; Xu, J.; Li, F.; Yi, T.; Huang, C. *Tetrahedron* **2007**, *63*, 6732.

(25) Song, K. C.; Kim, J. S.; Park, S. M.; Chung, K.; Ahn, S.; Chang, S. *Org. Lett.* **2006**, *8*, 3413.

(26) (a) Nolan, E. M.; Racine, M. E.; Lippard, S. J. *Inorg. Chem.* **2006**, *45*, 2742. (b) Collange, E.; Flamini, A.; Poli, R. *J. Phys. Chem. A* **2002**, *106*, 200. (c) Nolan, M. E.; Lippard, S. J. *J. Mater. Chem.* **2005**, *15*, 2778. (d) Nolan, M. E.; Lippard, S. J. *J. Am. Chem. Soc.* **2003**, *125*, 14270. (e) Chapoteau, E.; Czech, B. P.; Gebauer, C. R.; Kumar, A.; Leong, K.; Mytych, D. T.; Zazulak, W.; Desai, D. H.; Luboch, E.; Krzykawaski, Bartsch, R. A. *J. Org. Chem.* **1991**, *56*, 2579.

(27) McClure, D. S. *J. Chem. Phys.* **1952**, *20*, 682.

(28) Yu, M.; Shi, M.; Chen, Z.; Li, F.; Li, X.; Gao, Y.; Xu, J.; Yang, H.; Zhou, Z.; Yi, T.; Huang, C. *Chem.—Eur. J.* **2008**, *14*, 6892.

(29) Li, G.-K.; Xu, Z.-X.; Chen, C.-F. *Chem. Commun.* **2008**, 1774.

(30) Ros-Lis, J. V.; Marcos, M. D.; Martinez-Manez, R.; Rurack, K. Soto. *J. Angew. Chem., Int. Ed.* **2005**, *44*, 4405.

(31) Sheng, R.; Wang, P.; Liu, W.; Wu, X.; Wu, S. *Sens. Actuators, B* **2008**, *128*, 507.

(32) (a) Chae, M.-Y.; Czarnik, A. W. *J. Am. Chem. Soc.* **1992**, *114*, 9704. (b) Czarnik, A. W. *Acc. Chem. Res.* **1994**, *27*, 302.

(33) Boiocchi, M.; Fabbrizzi, L.; Licchelli, M.; Sacchi, D.; Vazquez, M.; Zampa, C. *Chem. Commun.* **2003**, 1812.

(34) Nolan, E. M.; Lippard, S. J. *J. Am. Chem. Soc.* **2003**, *125*, 14270.

(35) Thiel, O. R.; Bernard, C.; King, T.; Dilmeghani-Seran, M.; Bostick, T.; Larsen, R. D.; Faul, M. M. *J. Org. Chem.* **2008**, *73*, 3508.

(36) (a) Monahan, A. R.; Deluca, A. F.; Ward, A. T. *J. Org. Chem.* **1971**, *36*, 3838. (b) Gelbcke, M.; Masiala-Tsobo, C.; Parmentier, F.; Declerck-Grimee, R. *Anal. Lett.* **1980**, *13*, 975. (c) Fedorov, L. A. *NMR Spectroscopy of Organic and Analytical Reagents and Their Complexes with Metal Ions*; Nauka: Moscu; pp 37−39; (d) Olivieri, A. C.; Wilson, R. B.; Paul, I. C.; Curtin, D. Y. *J. Am. Chem. Soc.* **1989**, *111*, 5525. (e) Ibanez, G. A.; Olivieri, A. C.; Escander, G. M. *J. Chem. Soc. Faraday Trans* **1997**, *93* (4), 545. (f) Alarcon, S. H.; Olivieri, A. C.; Jonsen, P. *J. Chem. Soc. Perkin Trans. 2* **1993**, 1783.

(37) Saeva, F. D. *J. Org. Chem.* **1971**, *36*, 3842.

(38) Tamai, N.; Miyasaka, H. *Chem. Rev.* **2000**, *100*, 1875.

(39) (a) Patton, D.; Park, M.-K.; Wang, S. R.; Advincula, C. *Langmuir* **2002**, *18*, 1688. (b) Victor, J. G.; Torkelson, J. M. *Macromolecules* **1987**, *20*, 2241. (c) Reeves, R. L.; Kaiser, R. S. *J. Org. Chem.* **1970**, *35*, 3670. (d) O'Shea, K. E.; Kirmse, K. M.; Fox, M. A.; Johnston, K. P. *J. Phys. Chem.* **1991**, *95*, 7863. (e) Bigelow, R. W. *J. Phys. Chem.* **1975**, *79*, 2411. (f) Alizadeh, K.; Seyyedi, S.; Shamsipur, M.; Rouhani, S.; Haghbeen, K. *Spectrochim Acta Part A* **2009**, *74*, 691. (g) Rageh, N. M. *Spectrochim Acta Part A* **2004**, *60*, 103. (h) El-Gahami, M. A.; Khafagi, Z. A.; Ibrahim, S. A. *Can. J. Appl. Spectrosc.* **1991**, *36*, 108. (i) Kim, J. J.; Funabiki, K.; Muramatsu, H.; Shibata, K.; Kim, S. H.; Shiozaki, H.; Hartmann, H.; Matsui, M. *Chem. Commun.* **2000**, 753.

(40) (a) Grando, S. R.; Pessoa, C. M.; Gallas, M. R.; Costa, T. M. H.; Rodembusch, F. S.; Benvenutti, E. V. *Langmuir.* **2009**, *25*, 13219. (b) Iijima, T.; Momotake, A.; Shinohara, Y.; Sato, T.; Nishimura, Y.; Arai, T. *J. Phys. Chem. Sec. A,*. **2010**, *114*, 1603. (c) Chen, C.-L.; Lin, C.-W.; Hsieh, C.-C.; Lai, C.-H.; Lee, G.-H.; Wang, C.-C.; Chou, P.-T. *J. Phys. Chem. A* **2009**, *113*, 205. (d) Lukeman, M.; Wan, P. *J. Am. Chem. Soc.* **2002**, *124*, 9458. (e) Hsieh, C.-C.; Jiang, C.-M.; Chou, P.-T. *Acc. Chem. Res.*, **2010**, 10.1021/ar1000499. (f) Kim, C. H.; Park, J.; Seo, J.; Park, S. Y.; Joo, T. *J. Phys. Chem. A* **2010**, *114*, 5618.

(41) (a) Kasha, M. *J. Chem. Soc. Faraday Trans. 2* **1986**, *82*, 2379. (b) Douhal, A.; Kim, S. K.; Zewail, A. H. *Nature* **1995**, *378*, 260.

(42) (a) Chou, P.; McMorrow, D.; Aartsma, T. J.; Kasha, M. *J. Phys. Chem.* **1984**, *88*, 4596. (b) Nishiya, T.; Yamunchi, S.; Hirota, N.; Baba, M.; Hamazaki, I. *J. Phys. Chem.* **1986**, *90*, 5730. (c) Wu, Y.; Peng, X.; Fan, J.; Gao, S.; Tian, M.; Zhao, J.; Sun, S. *J. Org. Chem.* **2007**, *72*, 62. (d) Sinha, H. K.; Dogra, S. K. *Chem. Phys.* **1986**, *102*, 337.

(43) (a) Chou, P.-T.; Yu, W.-S.; Cheng, Y.-M.; Pu, S.-C.; Yu, Y.-C.; Lin, Y.-C.; Huang, C.-H.; Chen, C.-T. *J. Phys. Chem. A* **2004**, *108*, 6487. (b) Cheng, Y.-M.; Pu, S.-C.; Hsu, C.-J.; Lai, C.-H.; Chou, P.-T. *ChemPhysChem* **2006**, *7*, 1372. (c) Shynkar, V. V.; Mely, Y.; Duportail, G.; Piemont, E.; Klymchenko, A. S.; Demchenko, A. P. *J. Phys. Chem. A* **2003**, *107*, 9522. (d) Chou, P.-T.; Huang, C.-H.; Pu, S.-C.; Cheng, Y.-M.; Liu, Y.-H.; Wang, Y.; Chen, C.-T. *J. Phys. Chem. A* **2004**, *108*, 6452. (e) Chou, P.-T.; Pu, S.-C.; Cheng, Y.-M.; Yu, W.-S.; Yu, Y.-C.; Hung, F.-T.; Hu, W.-P. *J. Phys. Chem. A* **2005**, *109*, 3777–3787].

(44) Chattopadhyay, A.; London, E. *Anal. Biochem.* **1984**, *139*, 408.

(45) (a) Ozen, A. S.; Doruker, P.; Aviyente, V. *J. Phys. Chem. Sec. A* **2007**, *111*, 13506. (b) Fabian, W. M. F.; Antonov, L.; Nedeltcheva, D.; Kamounah, F. S.; Taylor, P. J. *J. Phys. Chem. Sec A,*. **2004**, *108*, 7603. (c) Kumar, M.; Babu, J. N.; Bhalla, V. *Talanta* **2010**, *81*, 9.

(46) (a) Rageh, N. M.; Abdallah, E. M. *J. Chem. Eng. Data* **2003**, *48*, 1495. (b) Zhao, M.; Samoc, M.; Prasad, P. N.; Reinhardt, B. A.; Unroe, M. R.; Prazak, M.; Evers, R. C.; Kane, J. J.; Jariwala, C.; Sinsky, M. *Chem. Mater.* **1990**, *2*, 670.

(47) de Silva, A. P.; Gunaratne, H. Q. N.; Gunnlaugsson, T.; Huxley, A. J. M.; McCoy, C. P.; Rademacher, J. D.; Rice, T. E. *Chem. Rev.* **1997**, *97*, 1515.

(48) (a) Lakowicz, J. R.: *Principles of fluorescence spectroscopy*, 2nd ed.; Kluwer Academic/Plenum Publication: New York, 1999; p 53. (b)

Misra, A.; Shahid, M.; Srivastava, P.; Dwivedi, P. J. Incl. Phenom. Macrocycl. Chem. 2010, 10.1007/s10847-010-9821-5.

(49) (a) Specht, A.; Bernard, P.; Goeldner, M.; Peng, L. *Angew. Chem., Int. Ed. Engl.* **2003**, *41*, 4706. (b) Huang, F.; Gibson, H. W.; Bryant, W. S.; Nagvekar, D. S.; Fronczek, F. R. *J. Am. Chem. Soc.* **2003**, *125*, 9367. (c) Huang, F.; Fronczek, F. R.; Gibson, H. W. *Chem. Commun.* **2003**, 1480.

(50) (a) Benesi, H. A.; Hildebrand, J. H. *J. Am. Chem. Soc.* **1949**, *71*, 2703. (b) Connors, K. A. *Binding constant*, 1st ed.; Wiley: New York, 1987.

(51) (a) Wei, F. S.; Qu, P. H.; Shen, N. K.; Fang, Y. *Talanta* **1981**, *28*, 189. (b) Johnson, D. A.; Florence, T. M. *Talanta* **1795**, *22*, 253.

(52) (a) Shimidzu, N.; Uno, T. *Chem. Pharm. Bull* **1978**, *26*, 127. (b) Shimidzu, N.; Uno, T. *Chem. Pharm. Bull.* **1977**, *25*, 2947.

(53) (a) Karipcin, F.; Kabalcilar, E.; Ilican, S.; Cagler, Y.; Cagler, M. *Spectrochimica Acta. Part A* **2009**, *73*, 174. (b) Shepherd, R. E. *Coord. Chem. Rev.* **2003**, *247*, 147. (c) Roy, R.; Chattopadhyay, P.; Sinha, C.; Chattopadhyay, S. *Polyhedron* **1996**, *15*, 3361.

(54) (a) Kurahashi, M.; Kawae, A. *Bull. Chem. Soc. Jpn.* **1976**, *49*, 127. (b) Kurahashi, M. *Chem. Lett.* **1974**, 63.

(55) (a) Mohamed, G. G.; El-Gamel, N. E. A.; Teixidor, F. *Polyhedron* **2001**, *20*, 2689. (b) Acuna-Cueva, E. R.; Faure, R.; Illan-Cabeza, N. A.; Jimenez-Pulido, S. B.; Moreno-Carretero, M. N. *Polyhedron* **2002**, *21*, 1961.

(56) (a) Kurahashi, M. *Bull. Chem. Soc. Jpn.* **1974**, *47*, 2045. (b) Kurahashi, M. *Bull. Chem. Soc. Jpn.* **1974**, *47*, 2067. (c) Ooi, S.; Carter, D.; Fernando, Q. *Chem. Commun.* **1967**, 1301. (d) Kurahashi, M.; Kawase, A.; Hirotsu, K.; Fukuyo, M.; Shimada, A. *Bull. Chem. Soc. Jpn.* **1972**, *45*, 1940. (e) Kurahashi, M. *Chem. Lett.* **1974**, 1271.

JP1049974